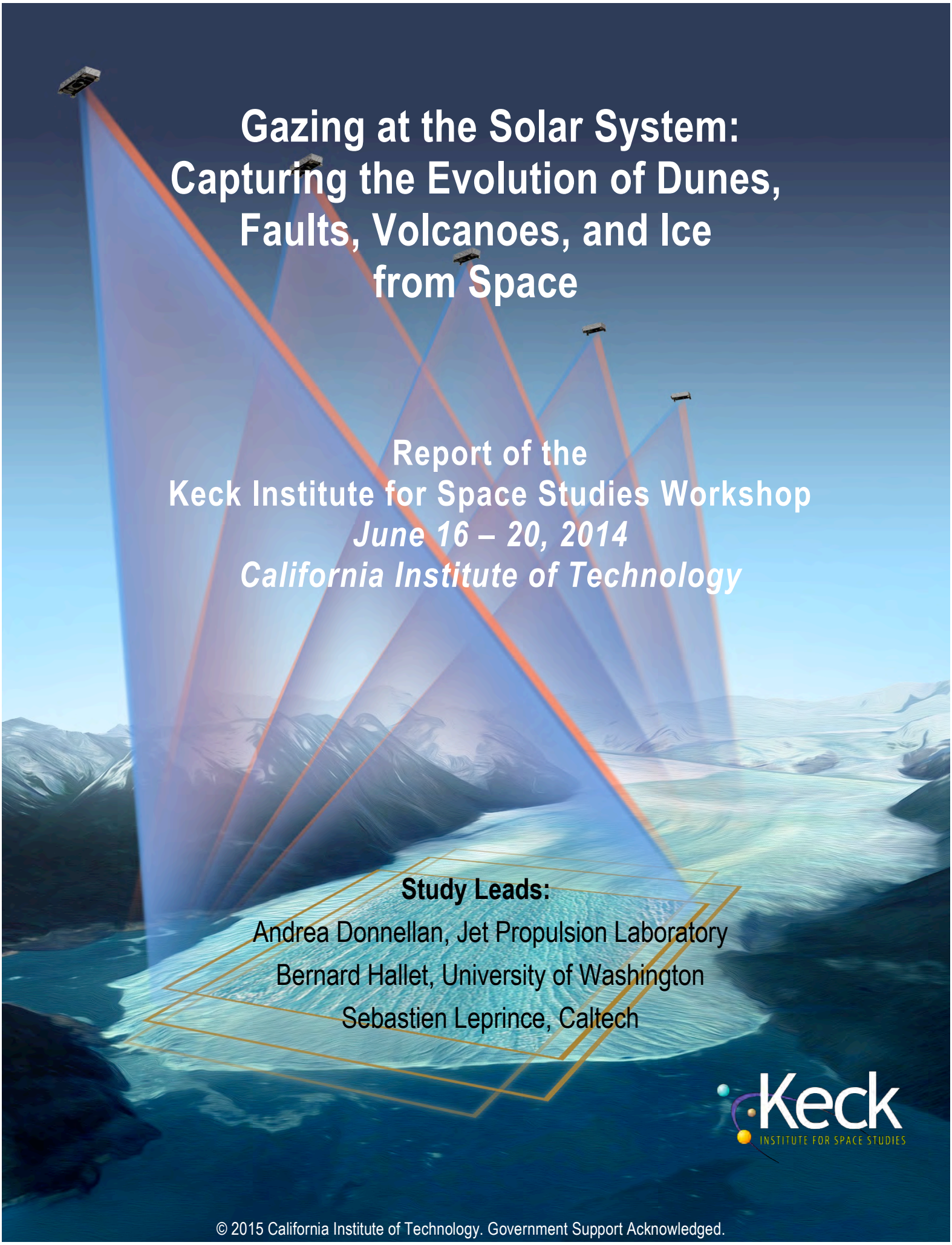

Gazing at the Solar System: Capturing the Evolution of Dunes, Faults, Volcanoes, and Ice from Space

Report of the Keck Institute for Space Studies Workshop

June 16 – 20, 2014

California Institute of Technology

Study Leads:

Andrea Donnellan, Jet Propulsion Laboratory

Bernard Hallet, University of Washington

Sebastien Leprince, Caltech

Keck INSTITUTE FOR SPACE STUDIES

Acknowledgments

During the week of June 16 – 20, 2014 scientists and engineers met to discuss the value of gazing imaging and possible observational strategies for a wide variety of applications. This report summarizes the results of the workshop.

The workshop was supported by the W.M. Keck Institute for Space Studies (KISS), the California Institute of Technology's Tectonics Observatory, and the Jet Propulsion Laboratory's Research and Technology Development Program under contract with NASA.

Workshop Participants:

Participant	Name	Institution	Expertise
Andrea	Donnellan	Jet Propulsion Laboratory	Hazards and glaciers
Bernard	Hallet	University of Washington	Geomorphology
Sebastien	Leprince	Caltech	Image science
Kate	Allstadt	University of Washington	Surface processes/seismology
Adnan	Ansar	Jet Propulsion Laboratory	3D reconstruction
Jean-Philippe	Avouac	Caltech	Tectonics and climate
Francois	Ayoub	Caltech	Mars imaging
Bruce	Bills	Jet Propulsion Laboratory	Geodynamics
Bodo	Bookhagen	UC Santa Barbara	Cryosphere and geomorphology
Nathan	Bridges	Applied Physics Laboratory	Planetary surface processes
Michael	Burl	Jet Propulsion Laboratory	Change detection
Bruno	Conejo	Caltech	Image Processing
Pablo	d'Angelo	German Aerospace Center	Image analysis
Eric	De Jong	Jet Propulsion Laboratory	Science visualization
Kevin	Franke	Brigham Young University	UAVs
Jay	Goguen	Jet Propulsion Laboratory	Photometry
Renaud	Goullioud	Jet Propulsion Laboratory	Optical systems engineer
Joseph	Green	Jet Propulsion Laboratory	Image science
Cyrielle	Guerin	CEA	Digital surface models
Simon	Hook	Jet Propulsion Laboratory	Hyperspectral
Nicholas	Lancaster	Desert Research Institute	Sand Dunes
Kiran	Murthy	Skybox Imaging	Spaceborne imaging
Amit	Mushkin	University of Washington	Earth/planetary geomorphology
Edwin	Nissen	Colorado School of Mines	UAS and structure from motion
Thomas	Painter	Jet Propulsion Laboratory	Snow
Ellen	Rathje	University of Texas	Disasters
Dirk	Scherler	Caltech	Glaciology and Remote sensing
Gunasekaran	Seetharaman	US Air Force Research Laboratory	Staring imaging
David	Shean	University of Washington	Structure from Motion
Joann	Stock	Caltech	Tectonics and volcanoes
David	Sutherland	University of Oregon	Ice/ocean interactions

Table of Contents

Introduction

Gazing imaging holds promise for improved understanding of surface characteristics and processes of Earth and solar system bodies. Evolution of earthquake fault zones, migration of sand dunes, and retreat of ice masses can be understood by observing changing features over time.

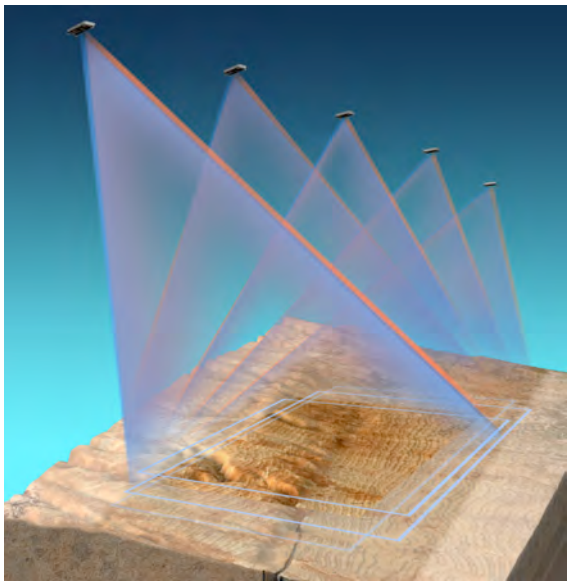

Figure 1. A gazing instrument would stare at and track targets from a range of vantage points during a single pass. For certain orbits solar illumination would vary between passes.

To gaze or stare means to look steadily, intently, and with fixed attention, offering the ability to probe the characteristics of a target deeply, allowing retrieval of 3D structure and changes on fine and coarse scales. Observing surface reflectance and 3D structure from multiple perspectives allows for a more complete view of a surface than conventional remote imaging. A gaze from low Earth orbit (LEO) could last several minutes allowing for video capture of dynamic processes. Repeat passes enable monitoring time scales of days to years.

Numerous vantage points are available during a gaze (Figure 1). Features in the scene are projected into each image frame enabling the recovery of dense 3D structure. The recovery is robust to errors in the spacecraft position and attitude knowledge, because features are from different perspectives. The combination of a varying look angle and the solar illumination allows recovering texture and reflectance properties and permits the separation of atmospheric effects. Applications are numerous and diverse, including, for example, glacier and ice sheet flux, sand dune migration, geohazards from earthquakes, volcanoes, landslides, rivers and floods, animal migrations, ecosystem changes, geysers on Enceladus, or ice structure on Europa.

The Keck Institute for Space Studies (KISS) hosted a workshop in June of 2014 to explore opportunities and challenges of gazing imaging. The goals of the workshop were to develop and discuss the broad scientific questions that can be addressed using spaceborne gazing, specific types of targets and applications, the resolution and spectral bands needed to achieve the science objectives, and possible instrument configurations for future missions.

The workshop participants found that gazing imaging offers the ability to measure morphology, composition, and reflectance simultaneously and to measure their variability over time. Gazing imaging can be applied to better understand the consequences of climate change and natural hazards processes, through the study of continuous and episodic processes in both domains.

Measuring Processes: A Need for Gazing

Natural hazards and climate change impact life and property worldwide. Understanding these phenomena enables better prediction of future behavior. However, this requires frequent high-resolution measurements of the changing surface in targeted areas around the globe in terms of its shape, spectra, and reflectance. A gazing approach, in which a target is observed from many vantage points, captures these measurements simultaneously in a way that cannot be achieved with existing systems. Natural target areas range from densely populated regions devastated by recent earthquakes, tsunamis, volcanoes, or landslides to remote regions where arid lands or glaciated mountains are responding progressively to climate change. More subtle targets include vast arid regions with changing surface texture from which dust enters the atmosphere, potentially impacting global climate, and of snow surfaces, for which dust and other aerosols impact the energy balance. Gazing imaging can be used to study dynamics, flux, and energy of many different systems (Figure 2).

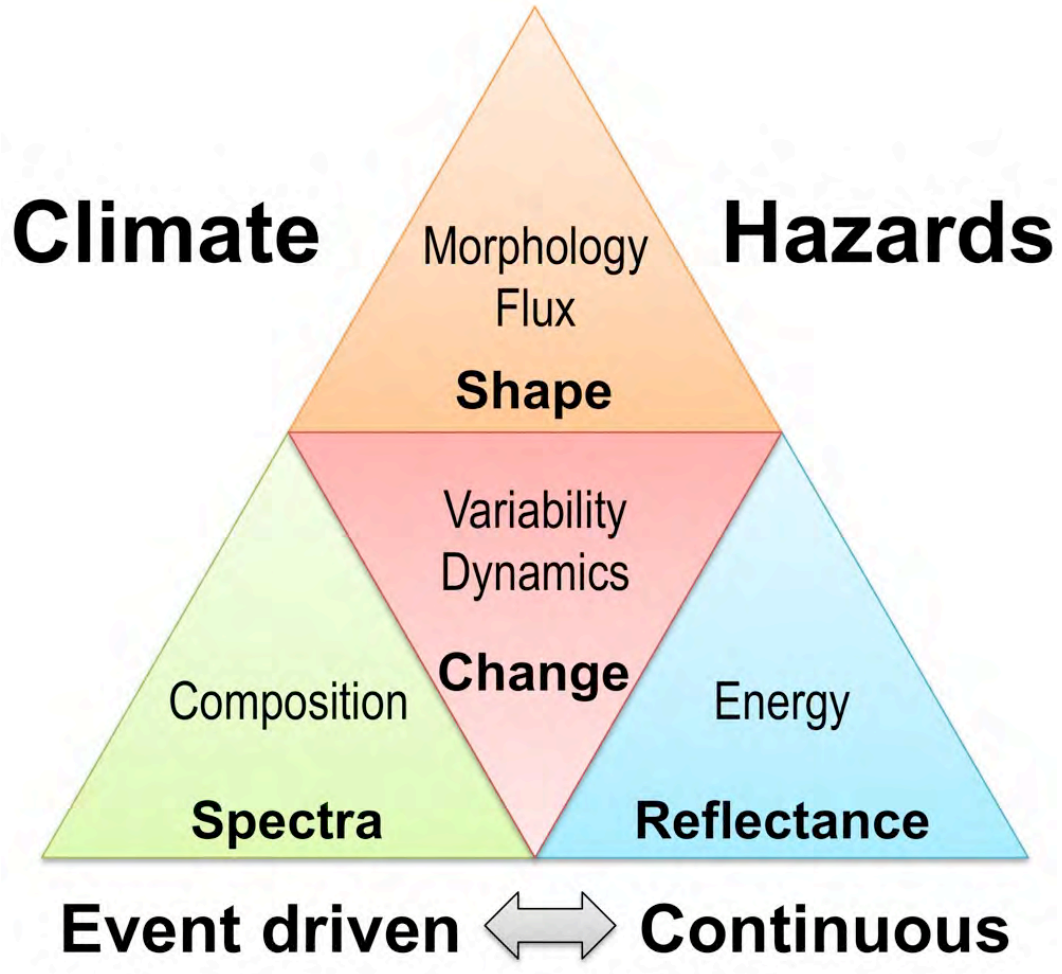

Figure 2. Major themes that emerged from the workshop that can be addressed using gazing imaging along with the types of measurements the method provides (in bold).

Measuring parameters simultaneously and their changes over time would provide unprecedented information about a variety of surface processes. The measurements address two fundamental questions:

1. What are the dynamic connections of Earth and planetary surfaces with their interiors and atmospheres?
2. What are the benefits of these insights into Earth and planetary surface dynamics?

Dynamic Connections

Our planet is shaped by dynamic interactions between its interior, surface, and atmosphere. Though these interactions have global reach, they can often only be characterized at relatively short length-scales and/or rapid time-scales – the slip in an earthquake, the retreat of a glacier, or the migration of a dune. We need to quantify changes to Earth's surface at higher resolution spatial and time scales in order to: 1) undertake strategic and focused long-term observations of processes using a consistent and reproducible measurement schema on a global scale, 2) improve our understanding of dynamic processes at all temporal and spatial scales, and 3) extrapolate event-scale observations to a global understanding of earth surface dynamics.

Climate Change

How do coastlines, lakes, rivers, glaciers, deserts, permafrost regions and ecosystems respond to climate change? Climate change impacts the world's supply of fresh water. Temperate-latitude glaciers and snowpack provide water for over one billion people dependent on ice melt water for continuous irrigation and hydroelectric power (Barnett et al., 2005). Thus, it is important to understand the influences of precipitation, temperature, solar input and surface contaminants on the spatial and temporal extents of snowpack. Permafrost degradation impacts roads and other structures and causes coastal-fluvial erosion. Changes in surface hydrology affect the exchange of carbon between soils and the atmosphere. Melting and thawing of permafrost releases sub-surface carbon dioxide, methane and other greenhouse gases into the atmosphere. Permafrost is the largest unknown of cryosphere processes. Rising temperatures also impact permafrost and vegetation processes that sequester carbon from the atmosphere. The complex interactions linking global climate, with land and ecological processes in permafrost regions are among the most elusive challenges in understanding climate change.

Glaciers

Multiple lines of evidence show that the Antarctic and Greenland ice sheets have been losing mass at an increasing rate over the past two decades (e.g. Rignot et al, 2011). Understanding the nature, causes, and evolution of ice-sheet mass loss is critical for constraining estimates of corresponding contributions to sea-level rise. The mechanisms responsible for this loss include ice dynamics (i.e. increased discharge due to acceleration, thinning, and retreat of outlet glaciers) and surface mass balance (i.e. changes in accumulation/ablation). Recent studies of Greenland's large outlet glaciers (e.g., Jakobshavn Isbrae,

Figure 3. The Jaundhar Glacier, Himalaya. India provides an excellent example of the steep terrain and complex, debris-covered surface of many mountain glaciers. Downwasting of the glacier can be observed in the foreground, where the steep and over-hanging debris-veneered ice cliffs cannot be imaged with standard imagery (courtesy Dirk Scherler).

Helheim) show velocity increases of ~50-100% and thinning of ~10-25 m/yr over interannual to decadal timescales (Joughin et al., 2008). These dramatic changes have been attributed to a reduction in resistive stresses near the terminus (Pritchard et al, 2009). Processes operating at or near the calving front remain poorly understood, however, in large part due to a lack of repeat observations for critical parameters such as surface elevation, which can be used to derive calving front height above flotation. A gazing system would provide multi-view stereo images capable of providing high-resolution elevation data, even for a steep calving front and iceberg slopes.

Mountain glaciers and high-altitude ice caps are retreating rapidly in virtually every region in which they are found. By 2002 their retreat contributed about 20% to present-day sea level rise (Dyurgerov, 2003), but increased to 29±13% in 2003–2009 and is forecast to intensify further (Gardner et al., 2013). Glaciers can also pose flood and avalanche hazards in some areas. The approximately 100,000 temperate glaciers currently in existence are typically small and many, located within the remote interiors of remote mountain ranges, where they are difficult to access. Steep terrain and the complex surfaces of the glaciers, which manifest a complicated set of processes governing the energy exchange at the glacier surface, drive a need to observe glaciers closely, at the meter to sub-meter scale from many vantage points (Figure 3). Gazing imaging provides the opportunity to acquire these observations.

Knowledge of the changing mass balances of mountain glaciers and snow packs is crucial for mitigating impacts to water supplies, sea level, and hazards

from outburst floods and avalanches. Accurate prediction of future mass balance changes requires an understanding of the nature and rate of glacier response to various forcings. Changes in precipitation, temperature, solar input and surface contaminants contribute to glacier advance and retreat. A thin mantle of rock debris, dust or soot on ice surfaces primarily enhances melting because of its darkening effect; on the other hand a thick mantle primarily insulates the ice and slows melting. What is the crossover thickness, and what are the rates of melting under various thicknesses of debris, dust or soot?

Avalanches and winds contribute to glacier mass balance by transporting snow onto glaciers. Inputs of debris and snow are difficult to measure, and most estimates rely on simple models; actual observations at the source are rare, and steep slopes (as high as 60°) are poorly represented using conventional imagery. The mass balance of many glaciers is also sensitive to changes in reflectance due to the rock falls, avalanches, and wind-blown snow. Gazing imaging can better characterize these systems through direct measurements of reflectance and accumulation from avalanches, wind-blown snow and rock falls.

The dynamics of water near the terminus of outlet glaciers are key to understanding the role of ocean circulation and ocean temperature in ice loss from glaciers reaching sea level, but these areas are very difficult to access in the field. How are the ocean and glaciers coupled in that inaccessible zone where active calving and icebergs of all sizes prevent ship access? Upwelling plumes at the glacier terminus in ocean and iceberg melt, in and out of mélange, provide some insight. Icebergs of different dimensions respond to different levels of the water column resulting in different drift rates, freeboard, and velocity field. Gazing imaging provides a means of observing this inaccessible region and an opportunity to shed light on key processes at the interface between glacial and ocean sciences. Fluctuations of these glaciers that reach the sea and lakes are complex because they are sensitive to changes in temperature, circulation and water depth at the ice front; these characteristics control rates of submarine ice melt and calving. And yet these characteristics have only been measured near a handful of glaciers (e.g., Rignot et al., 2010).

A particularly promising application of multiple high resolution observations sustained for minutes on single targets from a gazing imager would be to measure iceberg drift rates and elevation in fjords. Size and drift of icebergs within a glacier fjord respectively reflect the maximum depth of water and the circulation at various depths in the fjords. This was well illustrated for one Alaskan glacier, LeConte, using time-lapse photography from a ground-based camera in by Motyka et al., (2013). They conclude that subglacial freshwater discharge is the principal process driving high rates of submarine melting at tidewater glaciers. This buoyant discharge draws in warm seawater, entraining it in a turbulent upwelling flow along the submarine face that melts glacier ice. These effects must be considered when modeling glacier response to future warming and increased runoff. Similarly, sustained imaging from a gazing imager could contribute greatly to understanding the rapid disintegration of tabular

icebergs in the Southern Ocean, which share similarities with the break-up of ice shelves (Scambos et al., 2008).

Sand Dunes

Climate change can destabilize sand dunes as vegetation diminishes. These sand dunes can migrate and threaten to overrun villages and cities. Sand dunes also provide particles for sand and dust storms, which are becoming increasingly common in the southwestern United States and other areas suffering from water shortages and drought. Aeolian dune systems transport sediment from source areas, via transport pathways, to sand seas and dune fields. They are prominent features of the landscape in low- and mid-latitude deserts, where they cover as much as 30% of the land area, in addition to many coastal areas at higher latitudes. Dune fields and sand seas are classified on a continuum from active and largely vegetation free to vegetation stabilized, which is determined by the interactions among sediment supply, availability, and mobility (Figure 4).

Reactivation of vegetation stabilized dunes and dune encroachment are recognized as significant environmental hazards in arid regions and many coastal environments, which are likely to be exacerbated by predicted future climate and sea level change (Hesp and Walker, 2013; Thomas and Wiggs, 2008). Dune encroachment on human settlements, agricultural areas, and infrastructure, such as roads, railroads, irrigation canals, and power lines, by migration or extension of dunes is a widely encountered hazard and requires expensive sand control measures (Watson, 1990). A modest increase of plant cover on the order of 15% stabilizes dunes, whereas a decrease in plant cover mobilizes them. High-resolution imagery is needed to examine the dynamics of these processes in relation to climate change and variability, such as from drought cycles, and periods of increased rainfall.

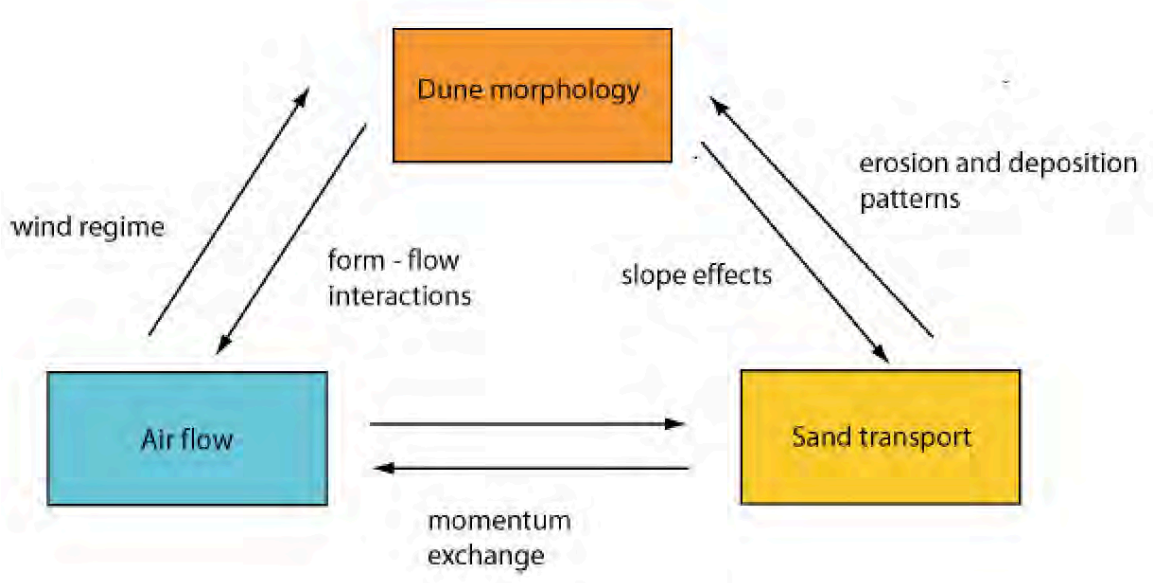

Figure 4. Fundamental processes of sand dune dynamics.

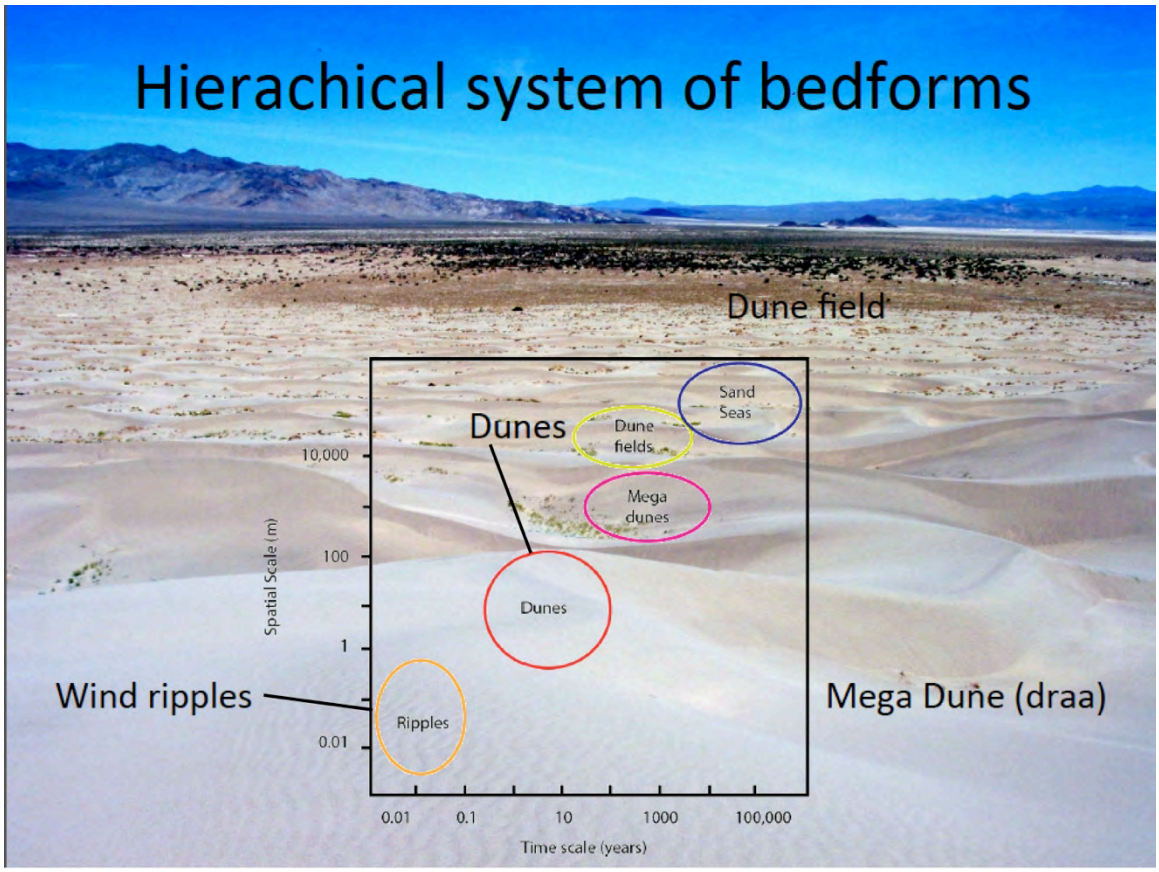

Figure 5. Hierarchical system of sand dunes and their scales. Gazing imaging would be best suited to studying wind ripples and dunes.

Recent work indicates that dune areas may play an important role in production and emission of aeolian dust (Figure 4), because they contain a reservoir of fine particles as a result of dust deposition and trapping by vegetation, pedogenesis, and abrasion of sand grains in episodes of strong winds and energetic sand transport (Crouvi et al., 2012). Reactivation of vegetated dune areas as a result of extreme drought and/or human disturbance may therefore release large amounts of dust (Bhattachan et al., 2012).

Changes in the area of active and largely vegetation free dunes have the potential to significantly influence regional climates, including positive feedbacks between land surface characteristics and the atmosphere (Nicholson, 2000), influenced strongly by the high albedo of active dune areas (Tsvetsinskaya et al., 2002) or by the favorable environment for vegetation growth provided by porous dune sands (Yizhaq et al., 2008).

Mineral dust in the atmosphere has implications for Earth's radiation budget, biogeochemical cycles, hydrological cycles, human health, and visibility (Parajuli et al., 2014). The patterns and rates of dust generation and sand transport are related to desertification. Dust generation depends strongly on the type of land cover. How do they vary with time and climate? What is the role of and impact on vegetation? It is difficult to detect and quantify change of rigid deformation,

plastic deformation, and changes in dune volume? Detection of wind ripples and their measurement is a limitation.

The shape of dunes is related to wind regime. Gazing imaging may make it possible to image dunes and wind ripples in a meaningful way (Figure 5). The measurements could be tied into sensitive measurements of winds at the surface that would provide boundary conditions for understanding the dune dynamics. Erosion and deposition patterns provide insight into sand transport. Wind ripples depend on wind speed, yet there are no systematic measurements of ripple migration on Earth, which may occur at rates of cm/hr. On Mars, ripple movement can be tracked because of their larger size and lower velocities compared to Earth (Bridges et al, 2012). Video from gazing imaging during a pass would be beneficial. Sun angle and shadowing may make it easier to detect ripples and other features on fine spatial scales.

Other Domains

Water bodies and coast lines

Shallow water and bathymetry can be imaged using color from multispectral data. Observation of thermal differences in the water surface, and changes in elevation and extent of inundation can be used to study circulation and overturn in lakes, and drainage events from below glaciers into rivers and lakes. Gazing multispectral imaging can be used to study lakes in Greenland, flow velocities of rivers, and river ice breakup, including in Arctic rivers.

Arctic lands are responding to global climate change (Intergovernmental Panel on Climate Change (IPCC), 2013). Along the ice-rich permafrost coastal bluffs of the Alaskan Beaufort Sea, this change manifests as rapid and accelerating coastal retreat of up to many meters per year (e.g. Barnhart et al., 2014). The presence of ground ice and the moderation of erosional processes by sea ice distinguish Arctic coastlines from their temperate counterparts and renders them particularly sensitive to climate changes. Along the central-western Beaufort Sea region 3–5 m tall permafrost bluffs with high ice content and fine sediment abut the shallow Beaufort Sea shelf. The coastal bluffs retreat by the incision of a notch into the base of the bluff, which subsequently causes bluff collapse. The composition and morphology of the coast allows efficient coastal retreat.

This coastline bounds the Beaufort Sea, which along with the Bering and Chukchi Seas is expected to experience some of the greatest future changes in the Arctic (Barnhart et al., 2014). Near-shore sea ice now disappears earlier in the beginning of the open-water season and open-water conditions persist longer into the autumn. The Arctic Ocean has warmed substantially, with sea surface temperature anomalies up to 5°C, and sea levels in the Russian Arctic are rising. Moreover, increased storminess in the winter and autumn is anticipated based on current coupled climate models. A multispectral gazing imager could significantly complement current studies of this Arctic coast erosion by imaging the ice-rich bluffs that also contain significant amounts of carbon and methane frozen in the

permafrost and the adjacent sea ice conditions, as well as monitoring coastal water temperatures in the circum-Arctic.

Other processes in coastal zones that could benefit from gazing imaging include: post storm recovery, the response of beaches to hurricanes and winter storms, and, erosion and sedimentation due to spatial variations in littoral drift along coastlines.

Ecosystems

Gazing imaging could be used to measure details of canopy height and vegetation thickness, complementing LiDAR measurements. Changes in ecosystems, such as from pine beetle infestations can also be measured. Changing angles from gazing imaging might offer advantages for seeing through obstructions from vegetation.

Animal migrations

Gazing imaging could also be used to monitor animal migrations and provide video. Examples include fishing stocks, whales, and large mammals.

Natural Hazards

Natural hazards occur unpredictably and can cause widespread damage and loss of life. They usually disrupt the Earth's surface or built environment. Accurate measurement of the disruption improves damage estimates and helps target emergency response. Gazing imaging can complement existing means of assessing disasters related to natural hazards and address questions such as:

- What conditions influence liquefaction and landslides?
- How is the coastline influenced by tsunamis, hurricanes, and sea level rise, and vice-versa?
- What are the causes and consequences of floods from large storms, rain-on-snow events, or glacial outburst?
- How are the magnitude and frequency of sand transport and dust storms changing through time?
- How does a volcanic eruption unfold?

Liquefaction

Liquefaction damages infrastructure. We can't accurately predict soil deformations resulting from liquefaction and as a result struggle to design resilient infrastructure. Measuring deformation associated with liquefaction from previous earthquakes can aid in predicting deformation and damage for future earthquakes. The spatial scale of liquefaction is 1–5 m and displacements are at cm scale. For instance, in the Colorado River Basin vertical motions of 1-2 m occurred in the 2010 M 7.2 El Mayor - Cucapah earthquake. The land surface was uplifted and sand and mud from mud boils was deposited, with lateral changes on a scale of 1 to several meters (Figure 6, left). Fields were no longer horizontal resulting in the loss of two harvests and 300,000 jobs in the agriculture industry. In the 1999 M 7.4 Izmit earthquake in Turkey, large apartment buildings

Figure 6. Left) Sand blows and liquefaction from the 2010 M 7.2 El Mayor – Cucapah earthquake. Right) fault scarp from the event (Fletcher et al, 2014).

tilted due to liquefaction. Gazing from low orbit could provide information on the timescale of liquefaction. Some examples indicate a delay of 30 minutes after the mainshock. Gazing could help address whether there is a delayed response, and whether liquefaction is triggered by aftershocks or pore pressure redistribution.

Landslides

Gazing could be used to monitor slow landslides and to identify unstable slopes that threaten human populations and infrastructure. Improving resolution is key. Images or video of a rapid landslide from a gazing instrument could be instrumental in advancing landslide science. Video or a high-resolution time-series of a rapid landslide would be extremely valuable in understanding landslide dynamics and the sequence of events. This information must currently be inferred indirectly and often with great uncertainty. Additionally, data from a gazing instrument could be used to calibrate and improve numerical landslide models, which are important for assessing landslide hazard. The main caveat of imaging landslides using gazing is that we rarely know where and when they will occur. However, areas could be targeted based on other events. Earthquakes trigger landslides directly due to shaking and often result in a post-seismic period of increased landsliding activity, so steep affected areas could be targeted afterwards. Landslide prone areas and known slow active landslides also could be targeted after heavy rains or fires.

Levees and Dams

Levee systems and dams are part of critical infrastructure. Gazing could be used to focus on areas of concern and monitor and inspect levees and dams for settlement, erosion, and cracks. Spatial resolution of 1m or better would be helpful. Thermal imaging might help detect incipient breaks in levees. Less than 1 m^2 of seepage area can take out a levee in under an hour.

Tectonics

Landscape features and surface deformation along active faults provide insights into faulting and tectonics. Complex fault damage zones range from a few meters to several hundred meters in width, but can extend for tens to hundreds of kilometers along the fault zone (Figure 6). The damage zone is difficult to observe with techniques such as Interferometric Synthetic Aperture Radar (InSAR), because the radar tends to decorrelate over the severely

disrupted areas, across the steepest deformation gradients, as well as in rugged topography. Gazing imaging could provide complementary detail to InSAR, GPS point measurements, stereo imaging, and LiDAR measurements. An earthquake can cause slip on numerous subsidiary faults that may lie tens of kilometers from the main rupture over a broad area, and which are easily missed from field observations. Slip on numerous faults occurred coincident with the 2010 M 7.2 El Mayor – Cucapah earthquake (Donnellan, et al, 2014, Rymer et al, 2011). By providing observations of topography and displacement at the required sub-meter scale, gazing imaging could be used to map earthquake slip, aseismic creep, aftershock deformation, and postseismic relaxation, all of which are key to understanding the mechanical and rheological properties of the fault zone and continental crust. Earthquake slip and subsidiary deformation is preserved in the landscape, where observations of topography and geomorphology provided by gazing imaging could be used to investigate historic and prehistoric earthquakes and deformation over multiple earthquake cycles (e.g. Zielke et al. 2010). Geo seismic imagers, a geosynchronous gazing instrument, may enable observations of ruptures as they form, as described later in this report.

Gazing imaging could be used to study overall plate boundary deformation. Iceland and Afar are two examples where oceanic rifts are subaerial and their ongoing behavior can be examined using remote sensing (Wright et al., 2012). These areas exhibit episodic rifting events, often progressing from dike intrusions and earthquakes to volcanic eruptions, which are difficult to observe along marine spreading ridges. Processes may take a few months and produce very large, measurable signals.

Volcanoes

Active volcanism occurs over a wide range of timescales. Dynamic processes range from longer-term deformation, dike intrusion, dome growth, lava flows, and ash cloud dispersal to the most hazardous extremely rapid processes such as explosions, eruption columns, pyroclastic flows, landslides, and lahars, while video capture could be used to study rapid processes. Unlike many other rapid natural hazards like earthquakes and landslides, volcanic unrest can often be anticipated through seismic, GPS, and gas monitoring. Furthermore, unrest can be long-lived, can be composed of multiple subevents of a variety of types, and often occurs in a relatively small target area. These factors make volcanoes an ideal target for a gazing instrument, which could be aimed where activity is likely to occur or already underway. This would allow for video capture and measurements of velocities of rapid processes associated with unrest like pyroclastic flows, lahars, and eruption column evolution. Images with such high spatiotemporal resolution could be revolutionary for improving our understanding of the physics behind all of these phenomena, as well as for improving and calibrating numerical models often used for hazard assessment. Repeat gazing imaging from many vantage points could be used to study slower processes such as bulging domes and other deformation.

Tsunamis

Earthquakes, landslides, and bolide impacts can trigger tsunamis. Tsunami models estimate wave propagation and timing within minutes of the detection of a potential tsunami-genic earthquake, and tsunami-monitoring systems are in place worldwide. These capabilities as well as the slower propagation times which can allow for the anticipation of the arrival of tsunami waves up to hours in advance make tsunamis a good target for a gazing instrument. Video and higher spatial and temporal resolution imagery could help improve our understanding of tsunami propagation and dispersion in shallow water, interactions with shore, and runup and velocity measurements.

Planetary Processes

Surface processes on many of the planets and satellites, such as Venus, Mars, Titan, Enceladus, and Europa, are very much like those on Earth. They include aeolian, fluvial, glacial and periglacial, impact, mass-wasting processes, tectonics, volcanism, and diurnal, seasonal and long-term climate change.

Systematic measurement of ripple migration on Martian sand dunes from a gazing instrument could provide unprecedented detailed information on fluxes, threshold wind speeds for entraining particles, seasonal effects, and ties to surface conditions and rover observations. Active dune fields, including the one about to be traversed by the Mars Science Laboratory rover Curiosity are ideal sites for repeat pass and gazing observations. Rates of surface modifications may be rapid.

Is there active tectonics on Mars? Some pit crater chains in Alba Patera may be actively growing due to active extensional faulting (Ferrill et al., 2004). Boulder fields and dust clouds from landslides may reflect recent earthquake activity on fault scarps at Cerberus Fossae on Mars (Roberts et al., 2012). Spagnuolo et al., (2011) reported that landslides and dune deposits in Aureum Chaos on Mars are cut by fresh-looking fault scarps. These locations would be natural targets for repeat pass observations or gazing at fault scarps.

Gazing Can Lead to Insights into Diverse Planetary Science Topics

- Aeolian dynamics on Earth, Mars, and Titan, including winds generating dust, moving sediments and eroding rock surfaces
- Dust lifting and storms - precise prediction of location and time
- Meteorological activity and dynamics in atmospheres of major planets Comparison of processes between planetary surfaces (e.g. Titan ‘rainfall’, erosion, and lakes)
- Behavior of ice covered with dust or rock debris on Earth and Mars
- Seasonal evolution of polar ice cap and active faulting on Mars
- Diurnal tidal flexing (100m bulge) and potential plate tectonics on Europa (Kattenhorn and Prockter, 2014)
- Outbursts on comets
- Io volcano activity and heat flow
- Short time-scale activity/change

Benefits of New Insights

Gazing imaging would complement current terrestrial remote sensing data, by providing more complete and high-resolution views of targets. This would eliminate bias in systems with one look and one illumination angle. It would simultaneously provide measurements that are currently derived from separate instruments with data collected at different times. Reflectance and changing structure is an example of such a simultaneous measurement. New observations promise to improve understanding of processes, which leads to improved prediction of behavior and hazards, and assessment of social and environmental vulnerability. This feeds into responsible and sustainable social and engineering practices that help develop strategies for dealing with, and adapting to, the consequences of climate change and hazards, and that improve the resilience of humanity. These consequences include changes in fresh water availability, storm surges and other effects of sea level rise, and impacts on roads and structures from permafrost degradation. They also include a rapid decline in sea ice in the Arctic with favorable consequences for navigation, shipping, and off-shore drilling activity, all of which would benefit from gazing imaging that would improve the monitoring of sea ice motion, freeboard, and fractures, with a focus on critical infrastructure.

Gazing imaging can also be used to address sustainability of agriculture and ecosystems. Observations can contribute to food security through improved understanding of droughts and changes in growing seasons. Ecosystem structure and biomass changes are measurable and related to carbon cycling. Habitats and migration patterns could be targeted for study, as systems are fragmented and degraded, or as environmental changes, such as from loss of sea ice, removing essential habitats quickly.

Gazing Imaging: A New Tool

Gazing imaging enables persistent, strategic imaging of processes and areas undergoing rapid changes. Varying view and illumination angles can be used to define surface reflectance, texture, roughness and small-scale topography. Surface motion and features can be tracked over single passes as well as over the duration of an operational gazing instrument. Gazing imaging is target focused; it is not a global mapping instrument. Instead the value of the instrument lies in observing a target repeatedly from many different vantage points with each observation lasting long enough to document certain active surface changes due to fast processes (discussed below). The instrument yields a more comprehensive view and improved understanding of the study target. Gazing instruments provide measurements that are complementary to broad area imagers.

Canonical Remote Sensing Telescopes

Most spaceborne imagers are designed for high-resolution wide area mapping with sporadic global coverage. Canonical remote sensing telescopes make use of pushbroom imagers, in which a scene is imaged with a linear array of pixels or multiple long arrays of pixels. The detectors are oriented perpendicular to the line of flight. Multiple rows operate in time delay integration (TDI) mode. The satellite ground track sweep forms the second dimension of an image. These pushbroom imagers are typically in low Earth orbit at 400–1000 km. They are implemented with a cascade of several Focal Plane Arrays (FPAs) with attached fixed filter to provide panchromatic and multispectral in any observational collection. (e.g. Table 1).

Table 1. Example operating pushbroom imagers and imaging characteristics.

Instrument	Number of Bands	Wavelength
MISR	9 different 4-band cameras at different viewing angles	VNIR
LANDSAT	7	VNIR, MWIR, TIR
ASTER	15	VIS, SWIR, TIR
WORLDVIEW-2	8	Pan + MSI: 400-1000 nm

In a pushbroom collection, the projected ground velocity of 7 km/s places a severe limit on integration time. To maintain a good signal-to-noise ratio (SNR) in the data, these linear arrays are actually implemented as narrow 2D focal planes to facilitate time-delay-integration (TDI), which successively builds up a signal as the imager sweeps over the target. Even with TDI, the systems are designed to be significantly undersampled favoring shorter integration times over maximizing the imaging resolution capability of the telescope.

The ratio of the resolution of the telescope to the sampling pitch of its detector is referred to as Q. Q is the ratio of the resolution the optical system presents to the focal plane to how finely the image is sampled. At Q=2, one fully maximizes

the optical resolution retained in the focal-plane sampled data. In practice, field of view, SNR and line-of-sight stability requirements often drive Q to lower values.

Q = 2 when pixel pitch = λ * f_number / 2 It is defined as

$$Q = \frac{\lambda \cdot F\#}{\Delta}$$

where λ is the wavelength of light, F/# is the ratio of the telescope focal length to its primary mirror diameter and Δ is the pixel pitch of a detector. When Q=2 there are 2 samples per maximum resolution element presented from the detector to the focal plane, maximizing the imaging resolution potential for that wavelength of light. In typical remote sensing systems, Q=1 for the panchromatic band and 0.25 for the multispectral channels. It is the only way to maintain good imaging SNRs while using short integration times to “freeze-out” the orbital velocity and minimize blur in its imagery. To make up the resolution loss due to low-Q, a larger telescope and/or a lower altitude of the spacecraft is needed.

Rotating the spacecraft during the collection slows down the sweep rate against a target and enables longer integration times but these act against the world mapping objective with area-rate-coverage being the primary driver. As such, pushbroom imagers tend to collect single to a few observations of a target in a pass as there are many other targets in the queue. It may take many orbits for a subsequent revisit.

Orthorectification is a key problem for such classic remote sensing. High precision orthorectification is required to relate images between different observation times and different sensors. Difficulty is driven by disparity in viewing geometry for high relief targets. Further complexity results from changes in scene content between revisits. When done well, orthorectification enables mosaicking, change detection, and data fusion.

Gaps with Current Systems

Current systems operate typically in fixed sun synchronous orbits. Because they are optimized for wide area mapping they generally do not observe a fixed target during a pass as this would take up half an orbital revolution sacrificing the ability to observe many targets. Wide area mapping is the priority rather than deep study of a target. Height recovery with current systems is typically accomplished from a two image stereo pair; the height resolution is good but not great. Occlusions, steep cliff faces, and surface properties, including texture, roughness, and albedo, are not thoroughly observed. Measurements designed to sample the specular geometry, which is rarely sampled by most orbiting instruments, could result in increased sensitivity to the state of the surface and improved energy balance estimates from orbit. A comparison of field and Landsat measurements shows a bias in glacier snow surface measurements (Klock et al, 2003), which may be due to the angular dependence of reflectance, and could be overcome with multi-angle gazing imaging.

Benefits of Gazing Imagers

Integration time

- Not limited with staring
- Can integrate up to a full second
- Non-sun-synchronous orbits
- Different Q - 1 ½ - 2
- Different ways of doing Pan and multispectral that doesn't sacrifice resolution
- Co-optimize telescope diameter with Q (not just a big light bucket to minimize integration time)

Continuity

- 1000s of images per scene
- New processing capabilities

Fast processes cannot be observed with broad area mappers that observe a target at most once per pass. The rate resolution would be on scales greater than or equal to days. Gazing imaging offers an opportunity to observe fast processes that occur on the timescale of a single pass. Such events potentially include landslides and avalanches, volcanoes, calving and motion of icebergs, ice break up on frozen rivers and lakes, and floods from glaciers carrying ice or other floods carrying woody debris.

Gazing Imagers

Gazing imagers enable fixed-point-staring imaging. The instrument rotates to maintain a fixed aim at the region of interest (ROI) during a pass. This cancels out principal ground motion relative to the camera. Images are acquired with a 2D focal plane array. Examples include Skybox, weather satellites, and cameras on the International Space Station (ISS). The method offers longer integration time than pushbroom imagers, the opportunity for non-sun-synchronous orbits, and ability to create videos of processes for a single pass as well as multiple passes. A non-sun-synchronous orbit allows for varying shadowing for a target, which can improve feature detection. Moreover, many processes change over the course of the day as the sun and temperature change, and a non-sun-synchronous orbit allows sampling these processes at different times of day. Gazing allows longer dwell time on a target, multi-angle measurements, and large off-nadir observations of steep slopes.

Long integration times of up to 1000 ms are possible for gazing imagers before residual blur becomes an issue. The primary ground track motion is canceled. Secondary dynamic effects from scene scale and rotation are slow. The system can be well sampled with a Q = 1.5–2.0 while maintaining a good imaging signal to noise ratio (SNR). $Q=\lambda*fn/PixelPitch$ where λ=wavelength and fn focal ratio or f-number. Both panchromatic and multi-spectral imaging modes can be well sampled. Integration time is free to be a variable in the design space (Figure 7). The improved signal to noise ratio reduces the constraint of needing

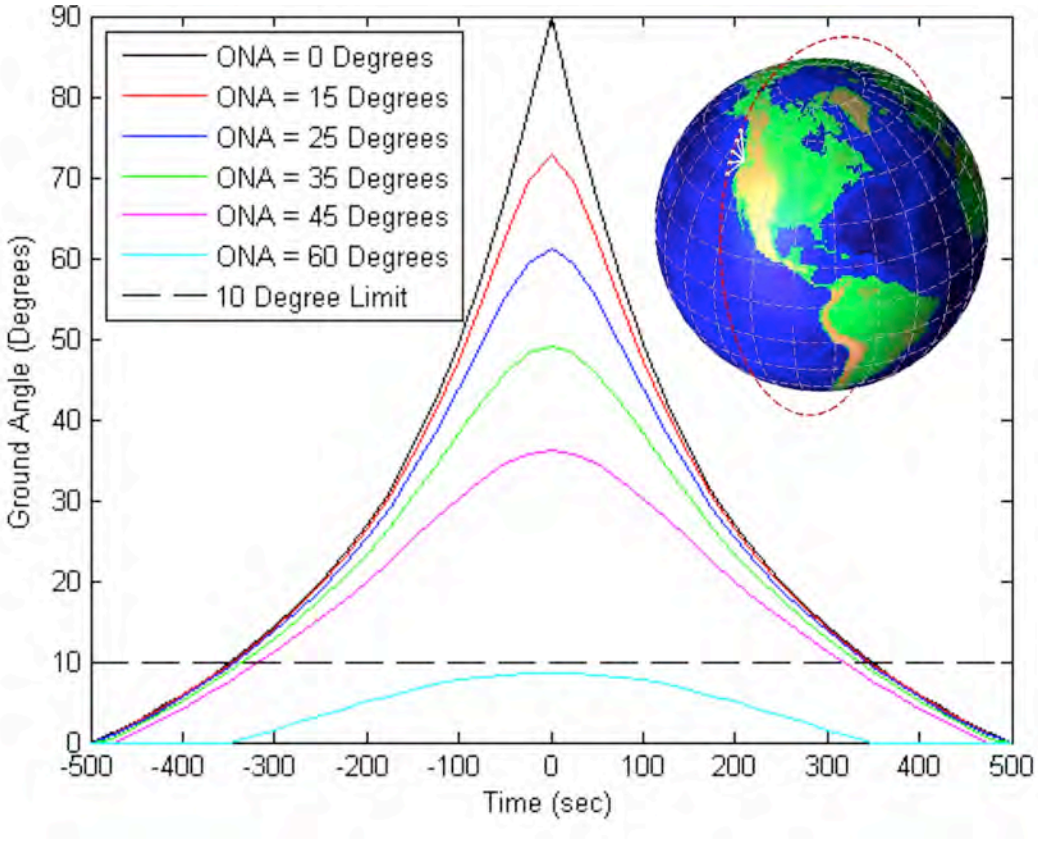

Figure 7. Dwell time on a target versus ground angle for different off nadir angles (ONA) with example fixed point stare on the globe.

to operate at high sun-elevation angles. The telescope diameter and altitude can be co-optimized with relaxed Q, leading to smaller telescopes flying higher to achieve the same resolution. The system can be optimized for persistence and continuous angle diversity. Collections can have hundreds to thousands of frames in a pass. Field of view is traded for the ability to delve deeply into the characteristics of a target.

Gazing imaging enables new processing capabilities such as:

- Automatic change detection, tracking, and flow measurements
- 3D reconstruction
- Sun and viewing angle induced effects for bidirectional reflectance distribution function (BRDF) estimation
- Multiframe super-resolution (sub-pixel resolution)
- High dynamic range imaging by exploiting a range of integration times to overcome finite focal plane array dynamic range

The automation of pass-ensemble data is straightforward.

Gazing imagers provide a unique operational and design space for telescopes due to long integration times, large ensemble SNR per pass, high level of continuous angular diversity, and a high Q that maximizes the data processing opportunities. Gazing imaging must be matched to the appropriate science applications that are target focused, not world mapping centric.

Table 2. Pushbroom versus gazing characteristics.

Feature	Pushbroom Imaging	Gazing Imaging
Integration time	0.1 – 3 msec (TDI)	Up to 1000 ms
Orbital constraints	Sun-synchronous (10 am – 2 pm)	Highly relaxed
Focal plane technology	1D Linear arrays (TDI)	2D focal plane arrays
Multispectral		
Implementation	Multiple linear arrays w/filters	Filter wheel, dichroics, bayer-filter,…
Imaging Q	0.25 – 1+ (optimized for int time)	Up to 2.0 (optimized for resolution)
Aperture diameter	Large to overcome low Q	Significantly smaller (matched to Q)
Frames per pass	1 – 10s	100s – 1000s
Field of view	Large (array + sweep limited)	Small (FPA limited)
Targets per orbit	Many 10s	2 – 10
Persistence on target	Very limited	4 – 10 minutes
Data quality issues	2D Image not rigid (sweep/LOS errors) Aliasing in imagery from low Q	Time-separation between bands Grain in images from high Q

Geo Seismic Imager

A gazing instrument in geosynchronous orbit would enable imaging surface motion of earthquakes in process. The Keck Institute for Space Studies (KISS) and JPL funded the study of a Geo Seismic Imager (Figure 8-9), which would be placed in geosynchronous orbit to continuously gaze at the Pacific Coast of the Americas. The objective would be to always cyclically record 10 minutes of high rate, high-resolution optical images. If an earthquake occurs then the data would be downlinked to provide a video of the propagating earthquake rupture and its surface wave field. Since it is not possible to know where and when the earthquakes will occur the instrument should have a wide range of view on the order of 300 km x 300 km. If an earthquake were to occur outside of the field of view the instrument could be retargeted to observe aftershocks from the event.

A geo seismic imager could be targeted at the Cascadia fault to observe episodic tremor and slip that occurs about every 14 months with a duration of several weeks. Geo seismic imaging could be coordinated with earthquake early warning, though moving rapidly enough to the target could be a technical challenge.

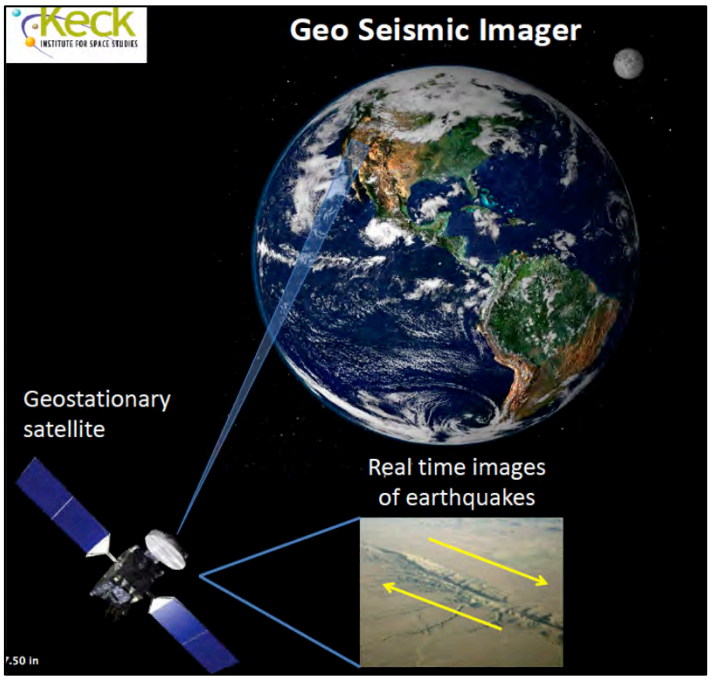

Figure 8. A geo seismic imager would gaze at the Earth from geostationary orbit. Image courtesy Jean-Philippe Avouac. Work was funded by a KISS/JPL study.

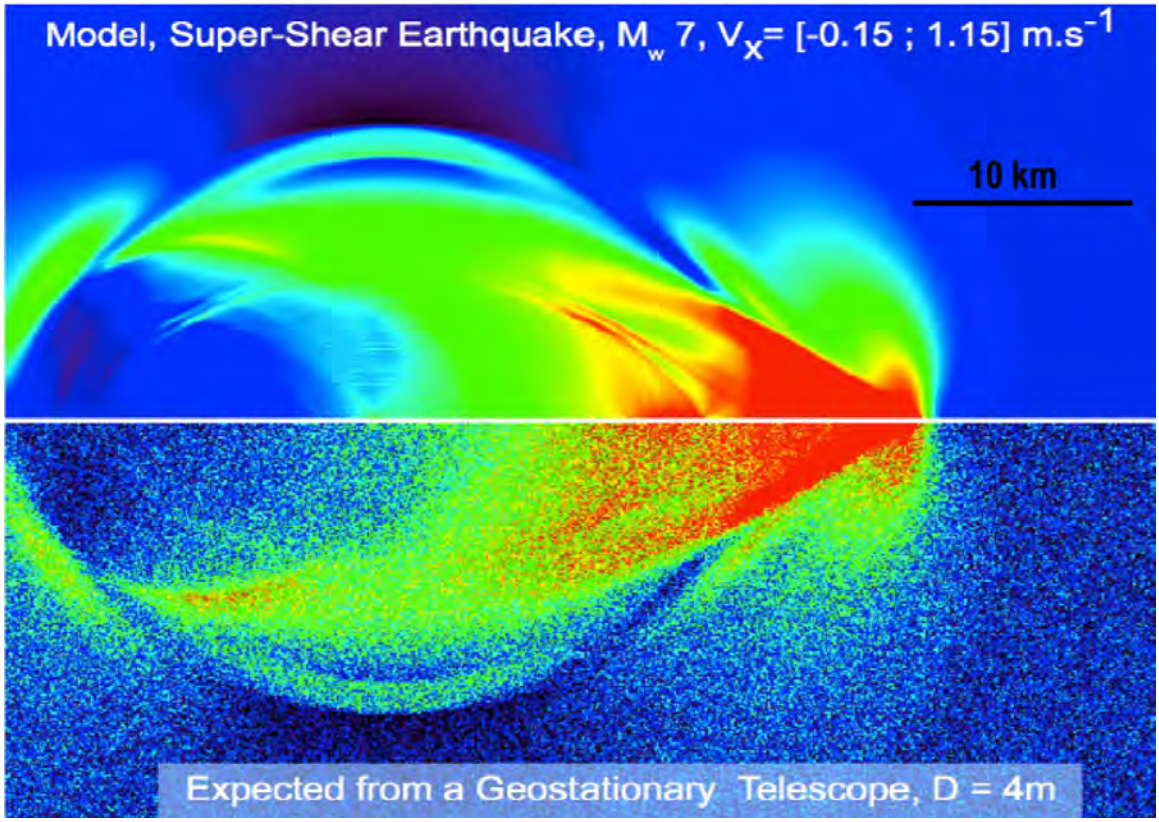

Figure 9. Top panel: simulated ground displacements caused by Mw 7.0 quake seen by a Geo Seismic Imager with a 4 m-diameter telescope. Bottom panel: simulation of ground displacements from the event as observed from a Geo Seismic Imager. After Michel et al (2013).

Science Needs

Gazing imaging provides the opportunity to observe fast surface processes as they are occurring providing insight into the physics of the processes. A geoseismic imager, for example, could provide valuable data on an earthquake rupture as it occurs (Michel et al. 2013). How faults rupture is modeled based on seismic data, or has been described anecdotally but rarely documented. Active volcanism, opening of dikes, and diverse geomorphic and glacial phenomena, are other natural targets for focused staring observations. Addressing the science requires systematic detailed coverage of key areas and features.

Gaps in Current Measurements

Remote areas, such as glaciers in the interior of mountain ranges, are difficult to access. This can cause a bias in the measurements and as a result it is not possible to define trends across geographic regions or mountain ranges. These interiors can be sampled by space-based imaging. However, clouds and high relief can cause occlusions in the measurements. Gazing imaging would make it possible to provide systematically distributed geographic measurements. It may make it possible to peer underneath clouds or cloud decks in some regions of the world. Clouds occlude some areas at certain times of day. A non-sun-synchronous synchronous orbit would enable sampling at times of day that have fewer clouds.

It is difficult to simultaneously measure multiple parameters using current systems. Instruments tend to be tailored to one or a few types of measurements. Gazing imaging offers the ability to simultaneously measure spectra, structure, and reflectance. Single look instruments can cause a systematic bias in measurements, particularly for surfaces that have a strong specular reflection at some angles. Gazing imaging samples many angles and strong specular reflections at some angles can provide information about the surface.

Rapid events can't be observed in detail with current systems. Skybox is an exception. Processes take place on many timescales ranging from sub-second to millennia. For example, dikes propagate, postseismic motions can occur rapidly, volcanoes erupt, and land can fail in landslides. Making measurements of these dynamic events as they occur will provide information about the underlying mechanics and the deformation.

Scales of Example Processes

Process	Temporal Scale	Spatial Scale
Sand dunes	-10 minute pass: with wind blowing. high resolution view of airflow patterns. Snapshot of wind ripples at one time. Possible over this time frame to get estimate of sand fluxes from wind ripple migration. Rates of lee side processes and avalanching. Provide synoptic view of transport events. -Monthly basis - wind events accumulate changes	~10 cm ripple wavelength changes on meter scale
Earthquake faults	<1 s to minutes coseismic, days to years for aftershocks and continuous postseismic, decades to centuries for interseismic	mm – m-scale coseismic mm-cm posetseismic mm/yr interseismic;
Dike intrusion (Iceland and Afar)	< 6 month (not steady state)	< 1 m
Pit chains on Mars	< decade	< 1 km
Mountain glaciers	Seasonal cycle, migration of snow line, and surface process and properties that control the atmosphere-glacier energy exchange, and hence the glacier mass balance. Large off-nadir observations are needed to image steep or overhanging icy-slopes.	< 1 m
Canopy height	Years	Cm to meters
Outlet glaciers	Crevasse formation and calving dynamics, outburst floods, surface subsidence and associated velocity anomaly	1m
Fjord oceanography and Icebergs	Motion of icebergs of different sizes reflects water motion at various depths in fjords, which is an important but rarely documented control on the melting of ice below the water line. Long gazing persistence on targets is most useful as top iceberg speeds are of order (1 m/min)	Icebergs from < 1 m to >10 m in diameter

Specific science needs

Temporal & spatial detail

Existing measurements of surface topography and roughness at the necessary sub-meter resolution are sparse, widely scattered, and not at sufficient temporal resolution to study and understand many surface processes and to extrapolate local insights to broader scales. In some fields, we have continuous point measurements at high temporal scales such as from seismic or GPS instruments and snapshot measurements at high spatial scales from existing satellite imagery, but there is a vast expanse in between. We need more persistent measurements to understand processes because interpolation can be difficult or impossible. Moreover with commonly used imaging capabilities, we are missing smaller scale roughness features. Imaging these must account for indirect radiation effects, effective albedo, and the strong influence of sun angle

and look direction. Careful consideration of the combination of look angle and sun angle is required for optimal imaging.

Studies of annual mass balance for alpine glaciers constitute a specific example of a field that could benefit greatly from better imaging systems. Observations of winter snow accumulation and summer snow/ice ablation are critical when attempting to estimate mass balance. Current approaches to obtain these measurements rely on costly field campaigns to dig snow pits and place survey stakes for a range of elevations on a few select glaciers. Remote sensing offers continuous spatial coverage over much larger extents. Repeat high-resolution DEMs can capture relative elevation changes with sub-meter accuracy, offering a direct measurement of snow thickness evolution and ice volume change over time. This technique can be applied to entire mountain ranges, offering near-real-time information for water resources management (e.g. Deems et al., 2013) and longer-term studies of inter-annual climate change. High temporal definition is useful for many glacier studies; for instance, weekly or monthly observations would be required to document seasonal changes, including snowpack growth and decay, and progressive ablation through warm periods.

Thermal imaging

While most of the discussion herein is focused on optical and topographic characteristics, much could be learned for focused imaging of the thermal dimension of the surface. Promising applications would include a number of processes, including:

- Near-surface dike intrusion (requiring visible to see movement - NIR - TIR. 0.1° resolution over short (10-min) time scales. How do the observed temperature changes correlate with topographic changes?
- Currents in lakes and shallow seas – How does the water temperature at surface change, and how does it reflect water movement?
- Thermal regime of ponds and lakes on glaciers and nearby marine waters – How does the water temperature influence melting processes on the surface of glaciers and terminus of tidewater glaciers? How does the temperature, as well as the turbidity of water near outlet glaciers reflect outburst floods? (e.g. Kjeldsen et al., 2014)
- Thermal state of Arctic coastline waters – How does it affect the extent and longevity of sea ice, and the rate coastal erosion in permafrost along the northern edge of circum-Arctic lands.
- Beyond earth: Are the flows that form gullies on Mars dry granular flows or wet debris flows? If they are wet, will they freeze and sublimate, rather then evaporate? What about newly formed craters and sub surface glaciers? Current data are limited by spatial and temporal resolution (CRISM - 18 m pixel scale) and are only collected during afternoon with sun-synchronous systems for Mars.

Table 3. Summary of measurement needs by discipline.

Discipline	Measurement	Coverage	Resolution	Response time	Repeat interval
Tectonics	Topography	10 km^2 (near field)	cm vertical	N/A	Single survey
Liquefaction	Topography and displacement Texture	100 km^2 to huge	cm vertical	< 10 min	2 days continuous coverage
Fault slip	Static displacement	2500 km^2	Few cm – m	Immediate	3 month continuous coverage (1s)
Earthquake	Seismic waves	10,000 km^2 (seismic waves)	cm – m	Concurrent	Irregular time between events. Continuous recording
Tsunami - interaction of wave with topography	Video providing Runup and water velocity	Coastal inundation	m	< hours	Irregular between events
Volcano	structure and thermal topography (deformation and eruption dynamics) velocities (flows, plumes)	25 km^2	0.1 - 10 m	Hours - days	<1 s (video - continuous is the important driver for fast processes) daily/weekly for deformation
Dune monitoring	Topography Roughness	10 km^2	Dunes: 1m vertical Ripples: 0.25 m vertical	N/A	Dunes: seasonal Ripples: hourly
Landslides Creeping	Topography, velocities	5 km^2	.1 m	N/A	monthly
Landslides catastrophic	Video	5x20 km	1 - 10 m	Hours	1s
Floods	Video Topography	100 km^2	1 - 10 m 1 m vertical	event based Hours to days	Yearly Once per day during floods
Levees	Topography Thermal	100 km^2 (?)	1 cm vertical Several meter posting		Yearly Once per day during floods
Fires	thermal	100 km^2	10 m	hours	N/A
Vegetation	multi-angle multi-spectral	100 km^2	meters spatial	day/weeks	seasonal
Dust storms	Topography roughness surface composition moisture content vegetation cover video	100 km^2	1 cm vertical for roughness 1 m horizontal for surface	event based (hours)	event based, gazing for duration of event

Discipline	Measurement	Coverage	Resolution	Response time	Repeat interval
Alpine glaciers	Topography Albedo, debris cover, temperature of surface ponds & lakes	1-20 km^2	0.1 m; < 75 degree off-nadir cone angles	N/A unless event	weekly
Outlet glaciers	Topography, iceberg motion, calving events, marine water temperature	1-100 km^2	10 cm vertical	N/A, unless event	weekly, high frequency (~1 Hz) imaging of termini for minutes
Mountain snowpack	Topography Albedo	1-10 km^2, multiple sites	cm vertical; <75 degree off-nadir cone angles	N/A	weekly
Snow Avalanches	Topography	1-10 km^2	1 m	Seconds	daily
Coastal erosion	Topography - including cliff-face, near-shore water temperature	5-10 km of coast line	1 m spatial 10 cm vertical	hours for storms	weakly - seasonal
Fluvial (river) erosion	Topography, river stage	1-100 km^2	1-10 cm vertical	N/A, hours for storms	seasonal, daily-weekly during events
Sinkholes	Surface subsidence and disruption	1 m ^{2}– 1 km^2	0.5 m	Hours	Baseline survey of prone area

Applications: Hazards and Surface Features

Better understanding is needed of the impact of multiple simultaneous hazards on large infrastructure systems, which could benefit substantially from improved imaging systems that target key areas of concern. Such systems can help scale up from individual eventsand local processes to regional and global patterns. The ultimate objective is to facilitate the translation of scientific knowledge and insights to policy and decision makers.

The science needs vary according to the many potential applications. A single application, the study of eolian dunes, is discussed here for illustration. The following staring imager observations of dune fields would be very instructive:

- 10 minute pass with wind blowing, yielding high-resolution view of airflow patterns, and snapshots of 10-15 cm wavelength wind ripples at one time. Rates of lee side processes and avalanching. Synoptic view of transport events.
- Repeated high-resolution topography. Changes of volume. Whole dune. Changes on event scale, and on meter scale. Ripples moving through dune field. Sand streamers (meter scale): how do they vary spatially and temporally?

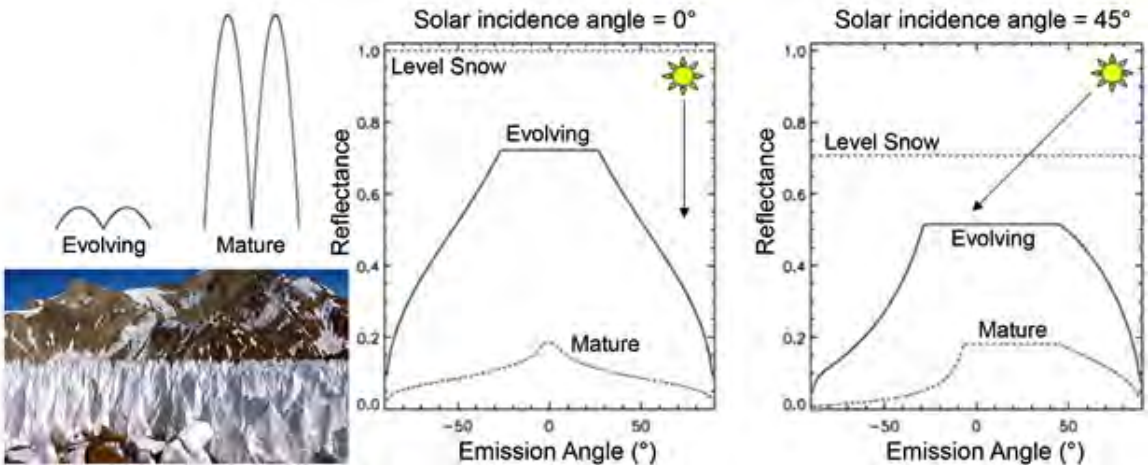

Figure 10. Evolving and mature ice pinnacle (penitentes) surfaces for solar incidence angles of 0° (*left plot*) and 45° (*right plot*) to illustrate extracting surface roughness from MUIR data. The height to width ratio is 0.5 and 5 for the evolving and mature models. The solid line is the reflectance that would be measured for the evolving model and the dash-dot line is the reflectance for the mature model. The dotted line shows a level snow or flat Lambertian surface.

Example: Gazing Applied to Glaciers

Gazing observations more fully measure snow, ice, or other surface characteristics. Knowledge of the angular distribution of the reflected light is essential to quantitative interpretation of remote sensing measurements in terms of the energy absorbed by the snow and available for melting. A resolution of 0.1-1 m is needed to measure current rates of thinning and retreat of glaciers. A field of view of 1 km is acceptable because most glaciers are < 1 km wide.

A simple ice pinnacle (or penitentes) model demonstrates that a rough surface causes a strong emission and incidence angle dependence of reflectance (Figure 10). The variation of reflectance with illumination and viewing geometry makes features such as ice and snow pinnacles, pooling water, wet ice, flat, and rough surfaces recognizable and quantifiable.

The angular resolution requirement from snow reflectance using laboratory observations of multi-angle measurements of different types of snow (Dumont et al, 2010) can be derived by examining the reflectance of ice with different albedos to understand the Bidirectional Reflectance Distribution Function (BRDF) for different illumination angles and vantage points. Results show an extreme geometry dependence of the reflectance that is most likely the result of a strong specular component in snow that needs to be incorporated into models for the BRDF of snow. Measurements designed to sample the specular geometry, which is rarely sampled by most orbiting instruments, could result in increased sensitivity to the state of the snow surface and improved energy balance estimates from orbit (Figure 11). The evidence for a strong specular component in the reflectance of even new snow opens up new possibilities for measurement strategies and potential for improving the interpretation of data from many Earth orbiting and aerial platforms investigating snow and glaciers. This can eliminate bias in current comparison of different data sets.

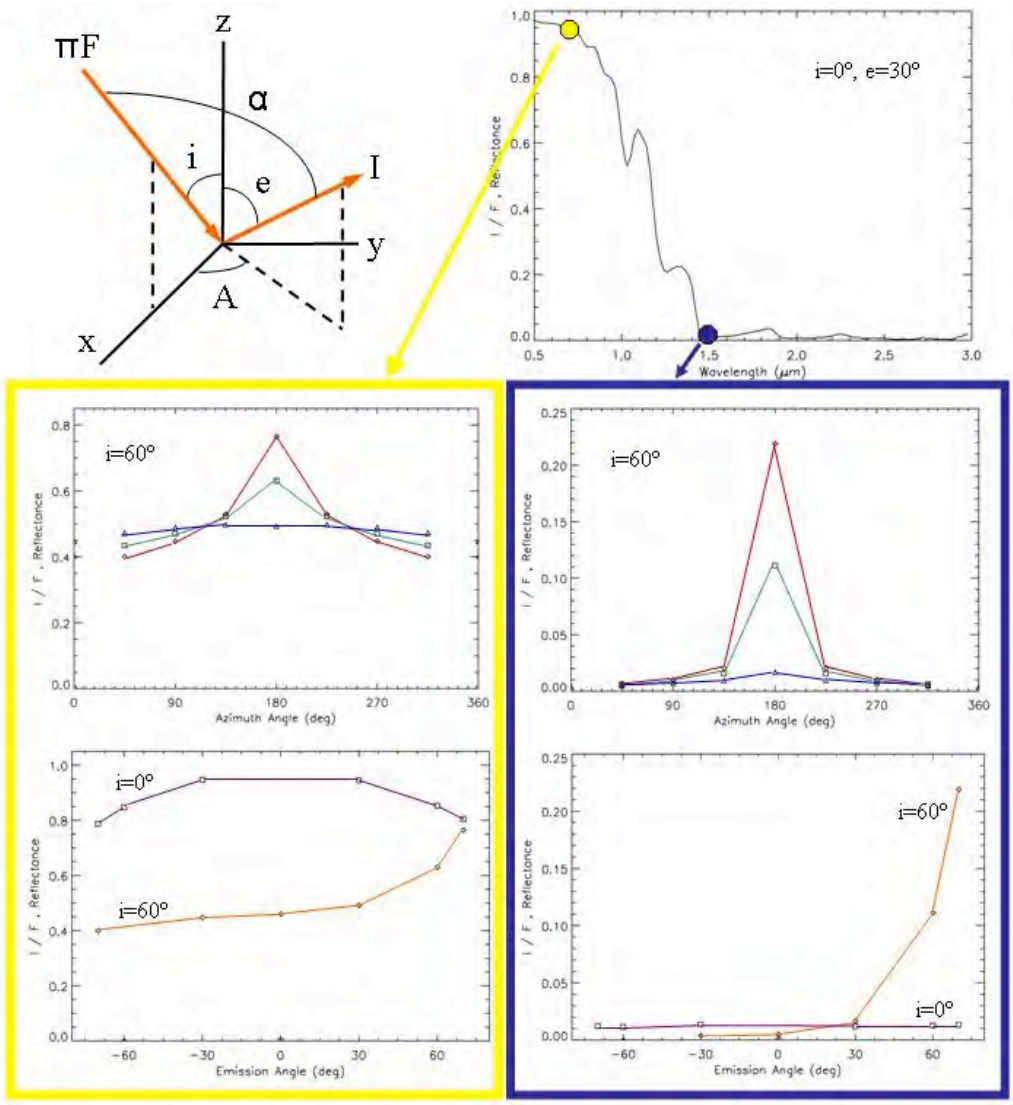

Figure 11. Top left: Definitions of incidence (i), emission (e), azimuth (A), and phase (α) angles used for analysis of Dumont et al (2010) measurements of new snow. Top right: Reflectance spectrum of new snow with high albedo (yellow circle) and low albedo (indigo) locations indicated. Bottom left: High albedo azimuth (top) and emission (bottom) angle dependence of reflectance of new snow. The peak at A=180º (top) is evidence that specular reflection is significant for the spectral range where albedo is high (colors: red e=70º, green e=60º blue e=30º. Bottom right: Same as bottom left, except for the low albedo case. Note the very strong A=180º (top) peak which is most likely due to specular (i=e, A=180º) reflection dominating the reflectance at this wavelength where the snow is strongly absorbing and is 'black' (I/F~0.01) at non-specular geometries. Recognition of this specular component is important for interpretation of remote sensing measurements of snow and glaciers.

BRDF models that include specular reflection can be developed and validated against the Dumont (2010) data set. Such models will make it possible to assess the potential of targeting specular geometries for snow and ice measurements that may provide improved sensitivity to snow age, snow surface physical state, and solar energy absorbed.

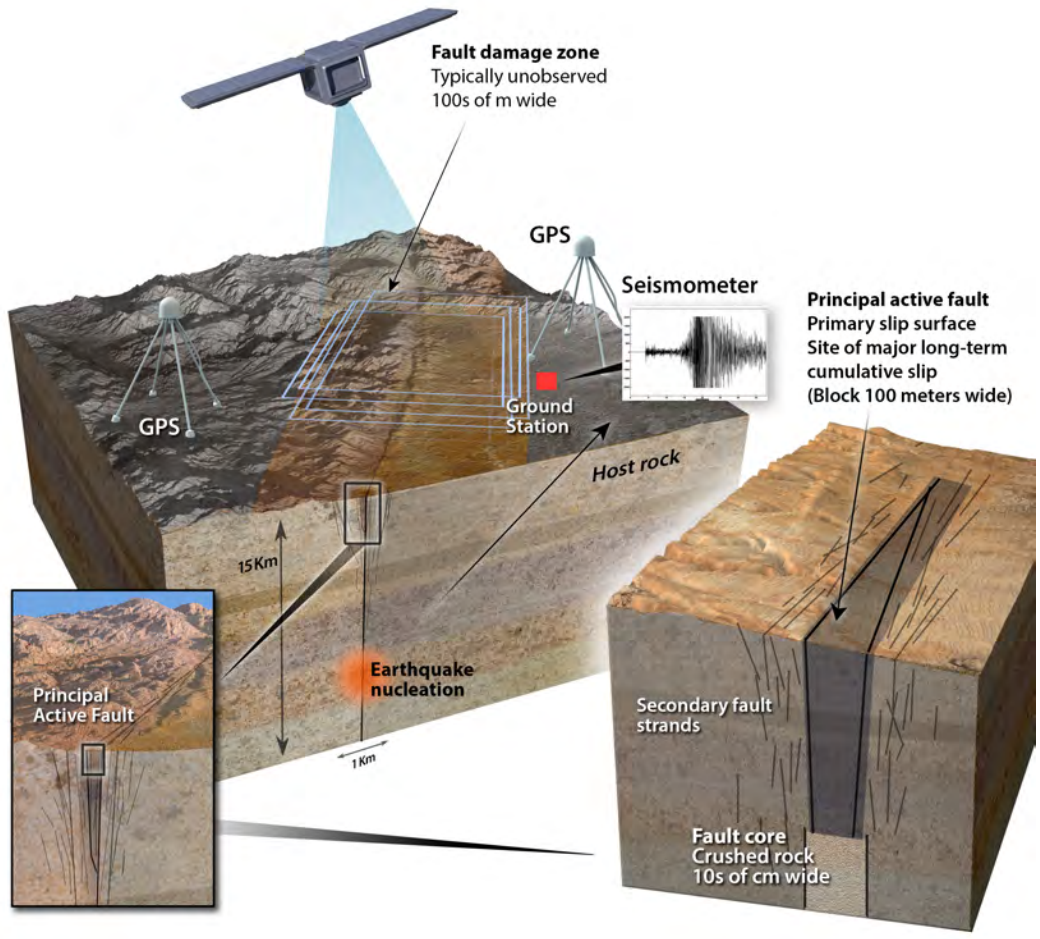

Figure 12. Earthquake fault zone showing the region that could be targeted with gazing imaging and other complementary measurements.

Example: Gazing Applied to Fault Zones

Most observations of earthquake processes and fault zones focus either on very short space-time scales of localized rupture and co-seismic data or on the far-field host rock, tectonic deformation, and interseismic period. With a few sporadic fortuitous exceptions, there is an almost complete lack of information on evolutionary properties and processes associated with intermediate time-space scales ranging from sub-minute to weeks and sub-meter to a few km (Figure 12). Gazing imaging can fill a gap of knowledge with high-quality space-based observations and use the data to build a more complete model for the physics of earthquake fault zones. Gazing imaging observations should be integrated with detailed seismological and geological observations of fault zones to provide a broad multi-disciplinary context for the results and application to less well-observed regions of the world.

Gazing imaging is complementary to other measurements, filling current gaps in resolution and view geometry necessary for observing steep slopes, disrupted areas, and surfaces with low contrast. Fault zones are difficult to study systematically. InSAR measurements decorrelate near earthquake faults. The

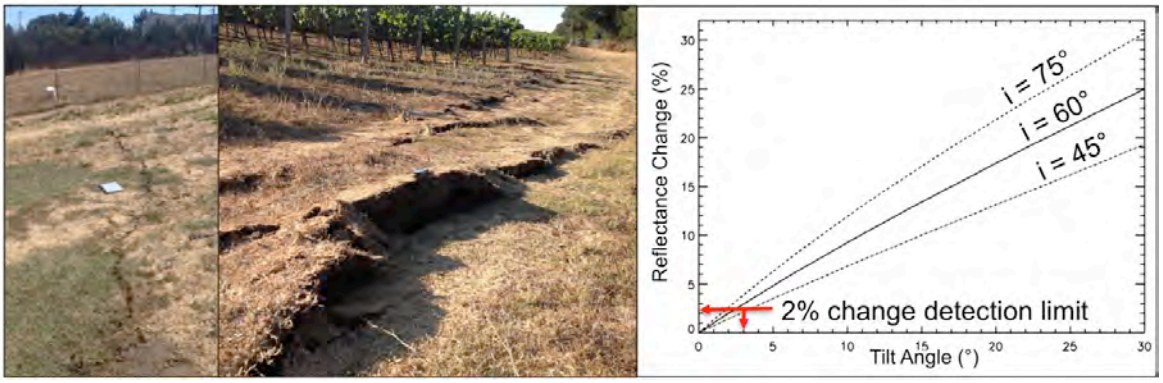

Figure 13. Photos) Cracks and en echelon fractures tilted by the mag 6.2 South Napa earthquake (from Hudnut et al, 2014). Right) Model change in reflectance for unresolved similar fractures with different tilt angles for three sun incidence angles measured from zenith. Similarly, cracks also reduce the reflectance.

number of faults in just California is too many to create a comprehensive dataset of details of the fault zones. Seismic observations can provide information about the fault at depth but little about aseismic and surface processes. Gazing imaging provides an opportunity to study the near-field details of earthquake fault zones.

Surface texture measured from directional radiance provides information about the fabric of a fault zone, which is ultimately indicative of the strength of the fault. Shadows may be sensitive to cracks parallel versus perpendicular to a fault, changes in vegetation due to water retention, or changing slopes of cracks. Volumetric changes can be estimated from crack density, granularity, and porosity of the rocks. Shear and tensile stress states can be inferred from surface anisotropy. How fluids migrate in fault zones can be inferred from estimates of permeability. A simple model calculation shows the effects of unresolved cracks and scarps on the average reflectance of a pixel (Figure 13). A reflectance change measured to 2% should be sensitive to tilted en echelon fissure scarps tilted as little as 3°. Cracks would effectively remove their area from the pixel, as long as the illumination isn't directly overhead, and the reflectance would change by their fractional coverage of the pixel area.

Dynamic rupture and recovery associated with an individual earthquake leave the traces of damage and rupture in the rocks and landscape of the fault zone. Characterizing the integrated effects of repeating earthquake processes on the landscape requires the fine scale imagery and decimeter topographic resolution that has hitherto been inaccessible in the synoptic, uniform, high quality form that gazing imaging could provide. The disruption of the landscape and the evident underlying geology is examined using these data in several ways: delineation of the belts of repeated rupture (e.g., Hudnut, et al., 2002; Arrowsmith and Zielke, 2009; Langridge, et al. et al., 2014); reconstruction of deformed landscape elements, such as stream channels, etc. (Frankel et al., 2007; Zielke and Arrowsmith, 2012; Salisbury et al., 2012), assessment of surface process response to repeated complex surface displacements (Hilley and Arrowsmith, 2008; Hurst et al., 2013) and characterization of fault zones (Milliner et al, 2015).

General Measurement Needs

Gazing imaging can provide the following measurements, needed to address a variety of scientific processes:

- 3D structure
  - Angular separation < 10° at ±60°
  - Decimeter level
  - Sub-weekly to continuous observations
- Dynamics
  - Flux
  - Variability
- Texture
  - Reflectance
  - 5-6 angles ±60°
- Composition
  - Multispectral bands
  - 2-3 visible
  - ~5 NIR
  - TIR

Limitations of Gazing

Gazing imaging is typically in the visible band and cloud occlusions can obstruct visibility of the target. Cloud ash, smoke, or haze can also make imaging difficult with optical methods. Adding SWIR or IR bands would help to mitigate this limitation.

Some processes occur suddenly making it difficult to be on target and capture the event when it occurs. Ongoing processes are easier to observe during a gaze. The episodic and unpredictable events that are hard to study under current methods would also be hard to study under a gazing system. Eventually, however, geosynchronous imagers could be deployed that continuously stare at regions of interest that are susceptible to rapid events.

As described earlier, low Earth orbit gazing imagers have a small field of view making them suitable for targeted measurements but not wide area mapping. Gazing imagers are complementary to wide area mappers and are not meant to replace them. Gazing imagers can have a large field of regard, however, providing agile access to various targets and science benefits from repeated measurement of a target from different vantage points over a single pass.

Algorithms, Techniques, and Approaches

During the last decade, several techniques have been developed to take advantage of multi-angle and multi-temporal optical imagery to characterize the Earth's surface morphology and its evolution. These techniques mostly aim at deriving accurate representations of the ground topography at a given time, and by comparing time-series of such data, they also aim at recording the potential deformation or erosion processes shaping the topography and the accumulation, ablation, and flow processes shaping ice masses. This section presents a review of several of these methods that could benefit a gazing system, as well as a discussion about their potential advantages and limitations.

Measuring 2D deformation using optical imagery

One of the early techniques developed to quantify morphological changes using satellite imagery is the correlation of multi-temporal orthorectified imagery. By finding the point of maximum correlation between small corresponding image patches, it was shown that horizontal ground movements could be tracked (Scambos et al, 1992). Initially mostly used to track glaciers because of the large displacements involved, the technique has, over the years, been made more robust and accurate; it is currently able to detect and track horizontal changes as small as 1/10 to 1/20 of the image pixel size (Van Puymbroeck et al, 2000, Leprince et al, 2007). These advances made it possible to monitor a wide range of other processes such as co-seismic displacement (Figure 14), landslide motion, sand dune migration (Figure 15), and lateral spreading due to earthquake-induced liquefaction (Leprince et al, 2008, Scherler D, et al. 2008, Scherler D, et al. 2011, Vermeesch and Drake 2008, Necsoiu et al. 2009, De Michele M, et al. 2012, Suncar et al, 2013, Kääb and Leprince, 2014).

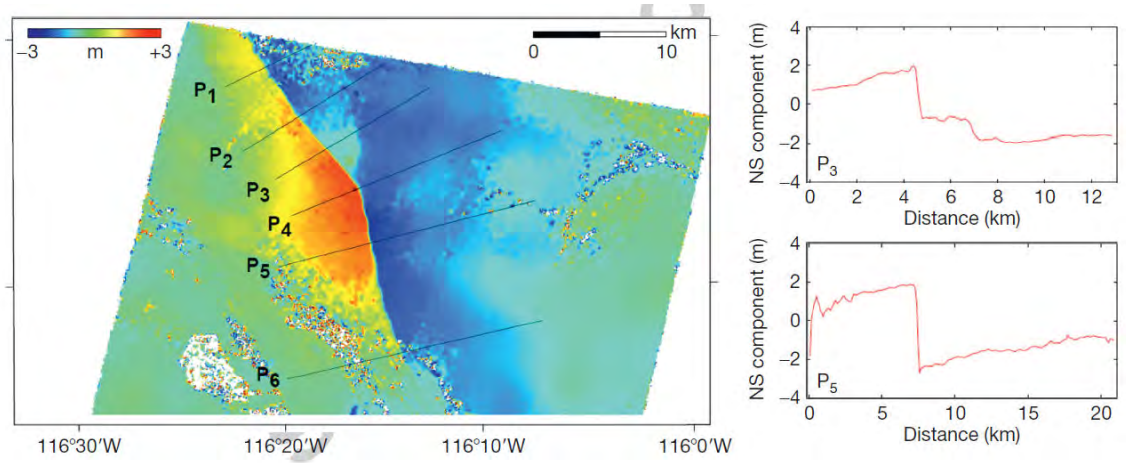

Figure 14: North component (positive to the North) of the coseismic displacement field due to the 1999 Mw 7.1 Hector Mine earthquake in California measured from correlating SPOT 2 and SPOT 4 monochromatic images with 10 m GSD acquired on 12 August 1998 and 10 August 2000. Both images were orthorectified and co-registered on a 10 m-resolution grid. Offsets were measured from subpixel correlation with a 32 x 32-pixel sliding window and a 16-pixel step. The offset field was denoised using the nonlocal means filter (Buades et al., 2008). The standard deviation on individual measurements is around 0.8 m. Right panels show 2 km wide swath profiles across the fault trace. These profiles show a clear discontinuity of surface displacement at the fault trace with up to 5.5 m right-lateral strike slip.

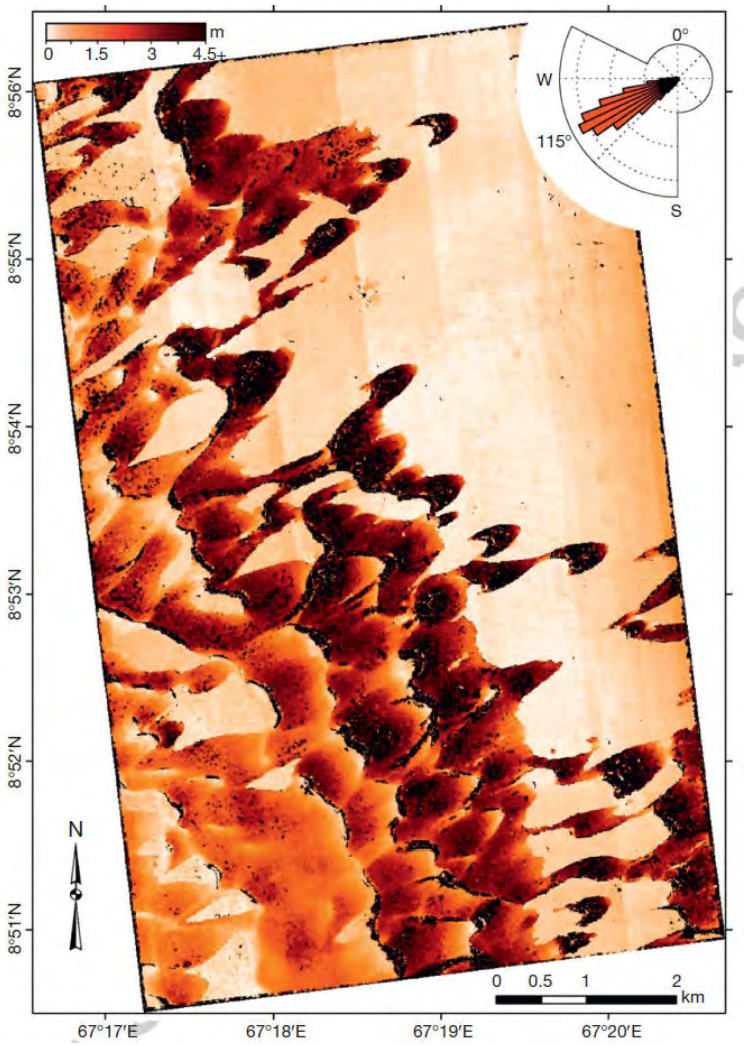

Figure 15: Amplitude of sand ripple migration in the Nili Patera dune field on Mars obtained from the correlation of two HiRISE images 3 months apart (Bridges et al., 2012). The wind rose in inset (upper right) represents the azimuthal distribution of ripple displacement vectors reflecting dominant winds blowing to the W-SW.

The main limitation of change detection from optical imaging is the need to produce accurate ortho-images, that is, images warped onto a topography model to remove parallax effects due to the acquisition angle. In addition to making the third dimension, i.e., the vertical, impossible to probe for changes using this technique, the insufficient quality of digital elevation models often fails to deliver accurate ortho-images when acquired with large incidence angles. In the absence of extremely good quality elevation models, regardless of the correlation accuracy, this technique is therefore limited to measuring horizontal ground deformation when images are acquired close to nadir, or with incidence angles differing by less than a few degrees (Figure 16).

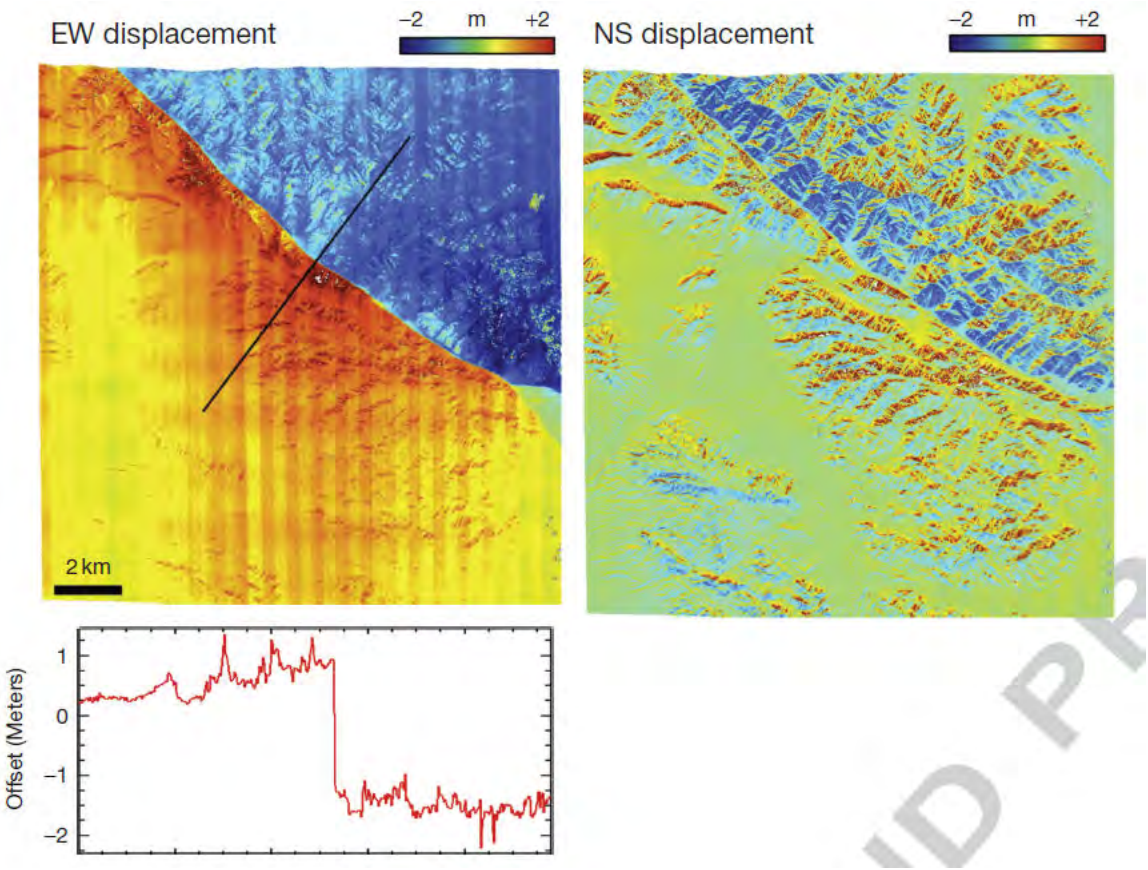

Figure 16. E–W and N–S surface displacements retrieved using only two WorldView images bracketing the 2010 El Mayor–Cucapah earthquake. Pre-earthquake image: WorldView September 2008 (along-track angle: -10.8° and across-track angle: 13.5°). Post-earthquake image: WorldView April 2011 (along-track angle: -13.8° and across-track angle: -22.5°). We see that large artifacts are introduced in the N–S component, which are due to topographic residuals along the epipolar direction (along-track sensor, which is mostly in the N–S direction). This example highlights the necessity of stereo acquisitions when images cannot be acquired at nadir.

Extracting 3D topography using stereo imagery

Techniques to extract the ground topography using at least two images acquired at the same time from different vantage points have been the focus of research for a number of years (Wolf and Dewitt BA, 2000, Scharstein and Szeliski, 2002). However, only recently the satellite technology has been providing imagery of sufficient resolution and satellites of sufficient agility to routinely acquire imagery capable of producing high quality elevation models. For instance, with a ground resolution around 31 cm, the Worldview 3 satellite can now rival airborne systems in the production of elevation data from multi-angle imagery (Worldview, 2014). Another example can be made of the new Skybox satellites (skyboximaging.com). Although the ground resolution is only about 1 m, the high sampling rate of the video mode allows the delivery of hundreds of multi-angle images above a site of interest, therefore, rivaling airborne multi- camera systems (Figures 17 – 19).

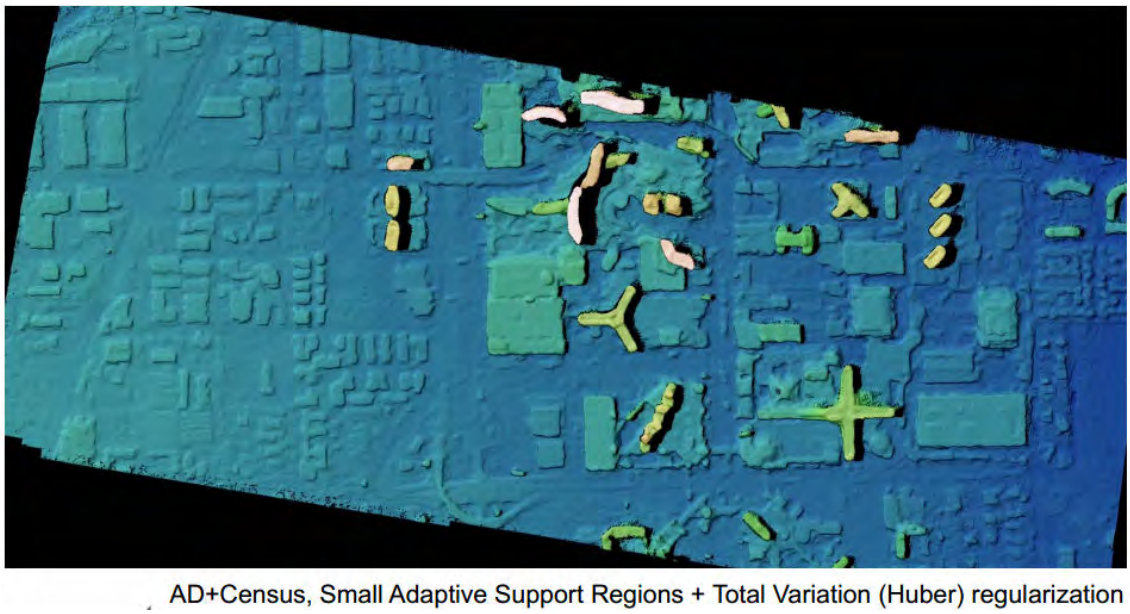

Figure 19. DSM extracted using 21 images (1 master and 20 slaves) from a Skybox sequence acquired above Las Vegas Extraction using semi-global matching and Total Variations (TV) regularization and median DSM stacking, courtesy of P. d'Angelo, DLR.

Structure from Motion (SfM)

Structure from Motion (SfM) is effectively an enhancement to binocular stereo imaging. Digital elevation models (DEMs) are refined through dense reconstruction by triangulation of corresponding points across multiple images (Figure 20). Each pixel in a reference image is assigned to a particular 3D plane or distorted DEM according to consistency across images with benefits of:

- Simultaneous (not pairwise) use of all data: No merging of pairwise results
- No need for pairwise rectification for near real-time performance
- Intrinsically better suited to wide viewpoint diversity
- Potentially better suited to handling occlusions

Measuring 3D deformation using multi-angle multi-temporal imagery

By merging both techniques to measure the 2D horizontal ground deformation and the 3D topography extraction, ground deformation can be defined quantitatively in 3D. As illustrated in Figure 21, this technique requires each event of interest to be bracketed by stereo-acquisitions. Figure 22 illustrates the application of the technique applied to several images bracketing the 2010 El Mayor-Cucapah earthquake, where for the first time the 3D displacement of the ground could be derived using optical satellite imagery. When the process of interest is continuous, e.g., glacier, landslide, dunes, the pairs of stereo images must be acquired simultaneously to avoid biasing the topography extraction. This constraint can be relaxed when studying potentially discrete events, e.g., earthquakes, but with the limitation that temporal decorrelation will increase the noise of the measurements. Recent agile and high-resolution satellite constellations should now, in principle, allow us to monitor the 3D evolution of a

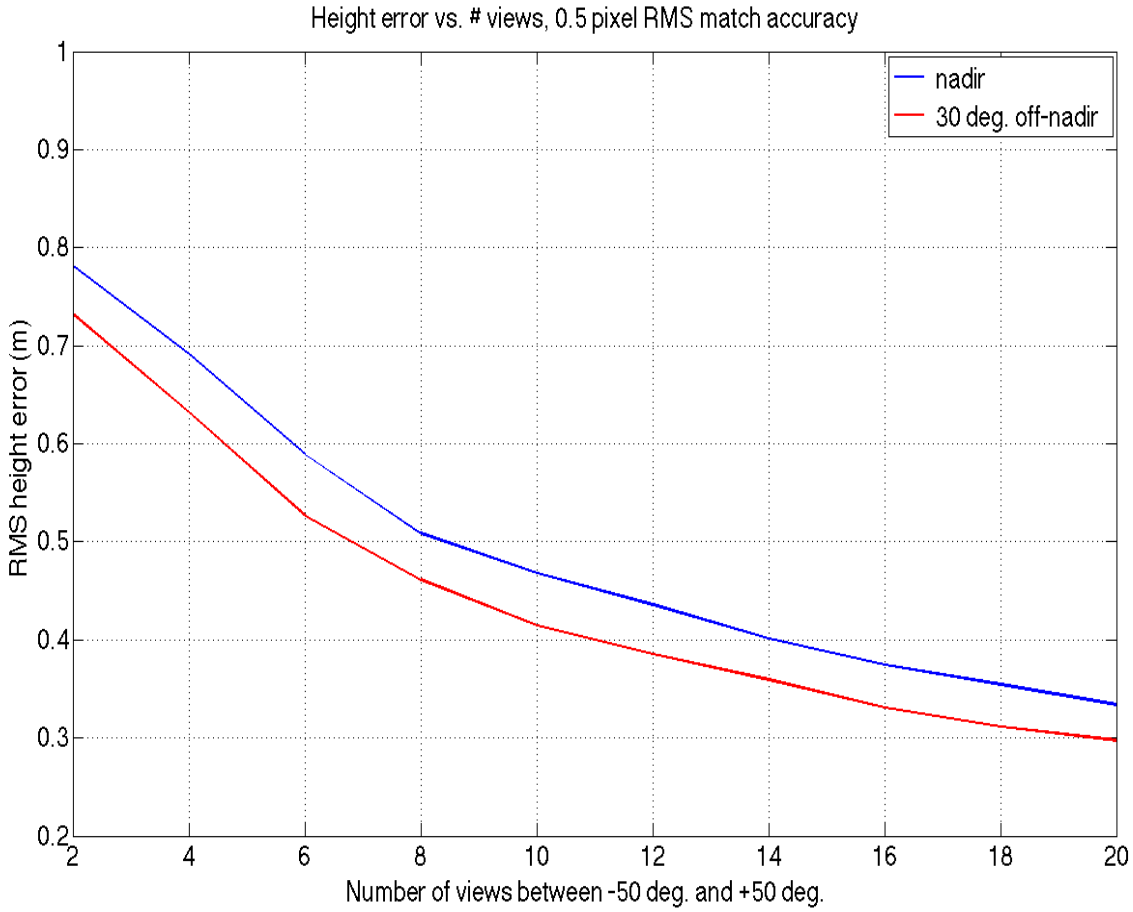

Figure 20. Monte-Carlo simulation for 12MP sensor at 0.3 deg FOV, at 400km orbit. 1σ simulated range resolution is shown as a function of number of views between -50 deg. and +50 deg. Nadir and 30 deg. off-nadir passes are shown.

wide range of surface processes. However, several limitations still exist, some pertaining to the nature of optical passive systems such as the limited visibility due to clouds or low light conditions; some others due to the matching techniques used, and the associated matching difficulties on steep slopes or when the ground is occluded by other objects; and some due to the nature of the scene changing in time due to seasonality or to the process to be imaged. Examples of the latter arise when the vegetation or snow cover changes, when shadows are moving, or when the ground features change due to a catastrophic landslide.

Errors in elevation have impact on: change detection, volume estimation, and ortho-rectification. Some of these limitations such as the visibility through clouds can be reduced by using SAR and equivalent satellite data, and using airborne surveys flying below the clouds, at the expense of not offering a global coverage of the Earth. When the ground presents poor visual texture to correlate on, extracting high-resolution topography from passive sensors might be challenging, and this limitation can be circumvented using an active system such as LiDAR.

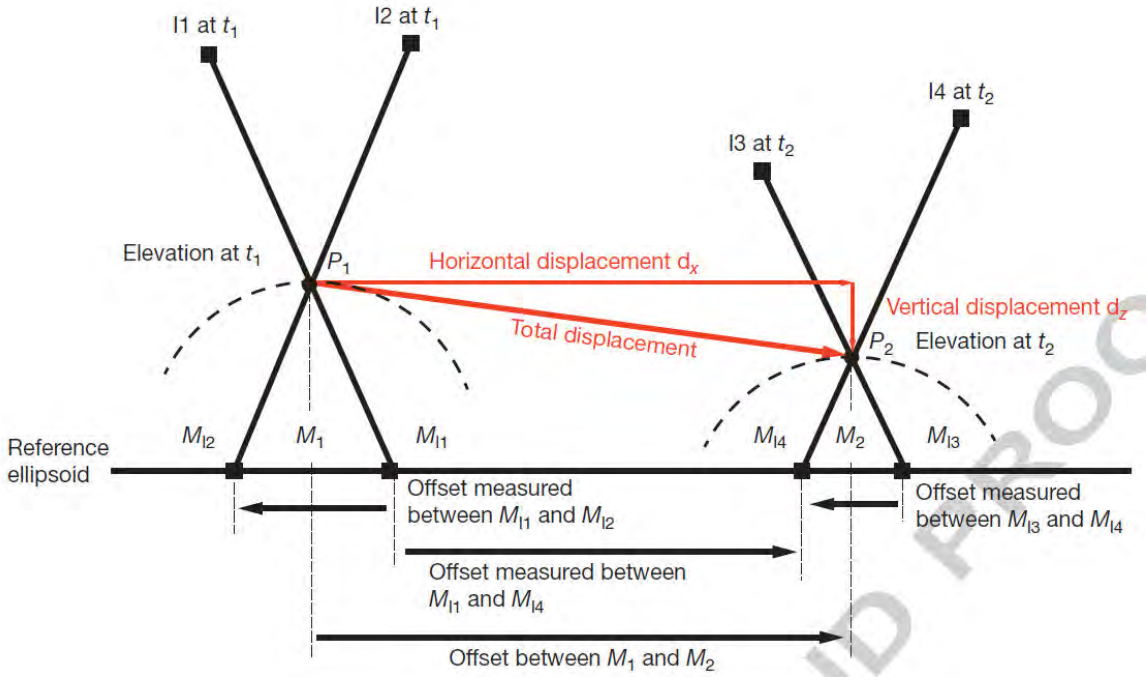

Figure 21. Given two pairs of stereo images (I1 and I2) and (I3 and I4), respectively, acquired at times t1 and t2, the 3-D displacement of a point P at the Earth's surface can be retrieved from the apparent offsets measured between each image pair projected onto a reference ellipsoid. Point P1, which lies at the Earth's surface, is projected at M1 and M2. After deformation of the Earth's surface, P1 is displaced to P2, which will be projected at M3 and M4 from images I3 and I4. Knowing the position of the optical center of the imaging systems using the imaging system ancillary data, the 3-D position of P1 and P2 can be triangulated, from which the 3-D displacement vector from P1 to P2 can be deduced. The procedure also yields a determination of the elevation of point P at epochs t1 and t2. If the elevations at epochs t1 and t2 are known or assumed, then the horizontal displacement is directly determined from measuring the offset between the orthoprojections M1 and M2 of point P at epochs t1 and t2. In that case, only two images are needed.

Measuring 3D change from multi-temporal LiDAR point cloud

As an active system, LiDAR offers the possibility of extracting high-resolution topography through direct measurement, without the need for image matching as for passive imagery. Therefore, topography models extracted from LiDAR are not subject to matching errors such as those generated on steep slopes, smooth ground, or biased from strong shadows. Successive LiDAR surveys can be differenced using cloud compare or similar software to reveal erosion and deposition patterns. LiDAR acquisitions are much less sensitive to atmospheric conditions such as cloud cover. Using full waveform LiDAR, it is also possible to distinguish the top from the bottom of the canopy, potentially making the analysis of LiDAR data less sensitive to vegetation changes. Moreover, in forested areas, LIDAR data can provide valuable information about aboveground biomass and vegetation structure. Finally, it is also possible to use the intensity of the LiDAR pulse returned to form an intensity image, which can be seen as a direct ortho image to be compared in time. LiDAR data therefore offer numerous advantages over passive optical imagery, but the main limitations arise from the cost of

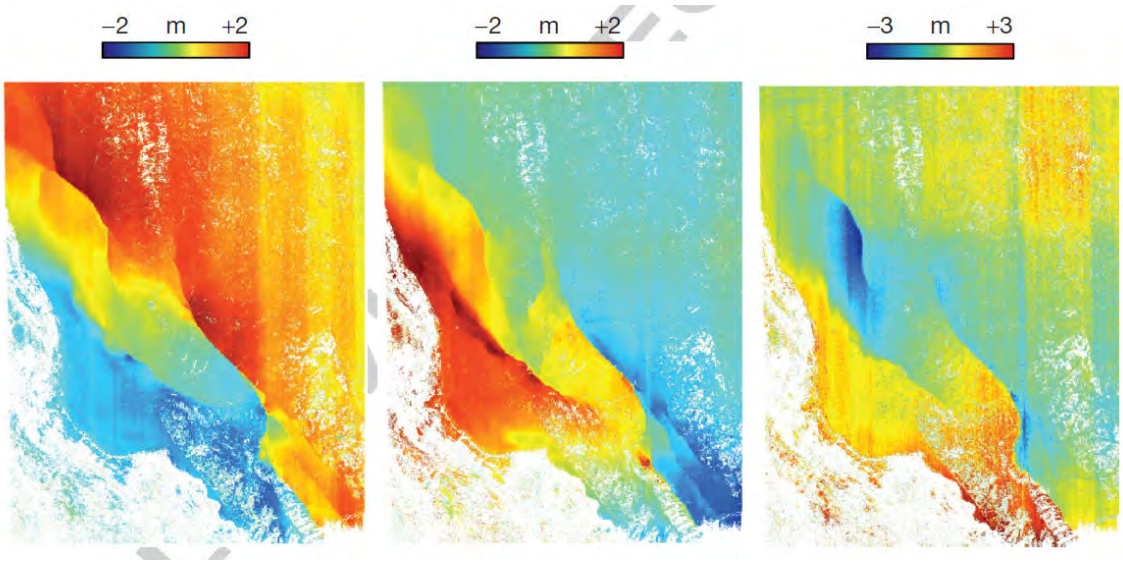

Figure 22. 3-D displacement field of the 4 April 2010, El Mayor–Cucapah earthquake retrieved using the method in Figure 19. Four images were used: pre-earthquake images, QuickBird 21 September 2006 (along-track angle: -1.23° and across-track angle: -9.8_) and WorldView 16 September 2008 (along-track angle: -10.8° and across-track angle: 13.5°) and post-earthquake images, WorldView 10 April 2011 (along-track angle: -13.8° and across-track angle: -22.5°) and WorldView 19 May 2011 (along-track angle: 14.1° and across-track angle 21.6°). Left, middle, and right images show east, north, and vertical components respectively.

operation, which is due to the cost of operating an active instrument. In addition, because it requires a lot of power, its use for high-resolution imagery is thus far only limited to low altitude airborne surveys. For these reasons, LiDAR data have thus far only been used for more localized studies, or when planning an airborne survey was not a limitation.

Having a direct measurement of the topography at different times, the evolution of the topography in 3D can be determined using two different matching approaches. The first approach simplifies the ground deformation to be separable between horizontal and vertical components. Then, a 2D matching algorithm, similar to the one used for stereo image matching, can be used to deduce the horizontal component of the deformation (Figure 23). Correcting the LiDAR data for this horizontal displacement field, the vertical displacement field can then be deduced by simple subtraction. The advantage of this formulation is its simplicity and low complexity. Because the horizontal deformation field results in a matching process but the vertical offset is measured using subtraction, the vertical offset field will have higher resolution than the horizontal offset field retrieved.

The second approach does not assume the displacement field to be separable and is more general. It is trying to directly match two topography surfaces in 3D, such that the 3D distance between the surfaces is minimized. Nissen at al. (2012) first show promising results using the Iterative Closest Point (ICP) algorithm. However, ICP does not guarantee that the deformation found is indeed the most likely deformation, but rather the deformation of shortest path to

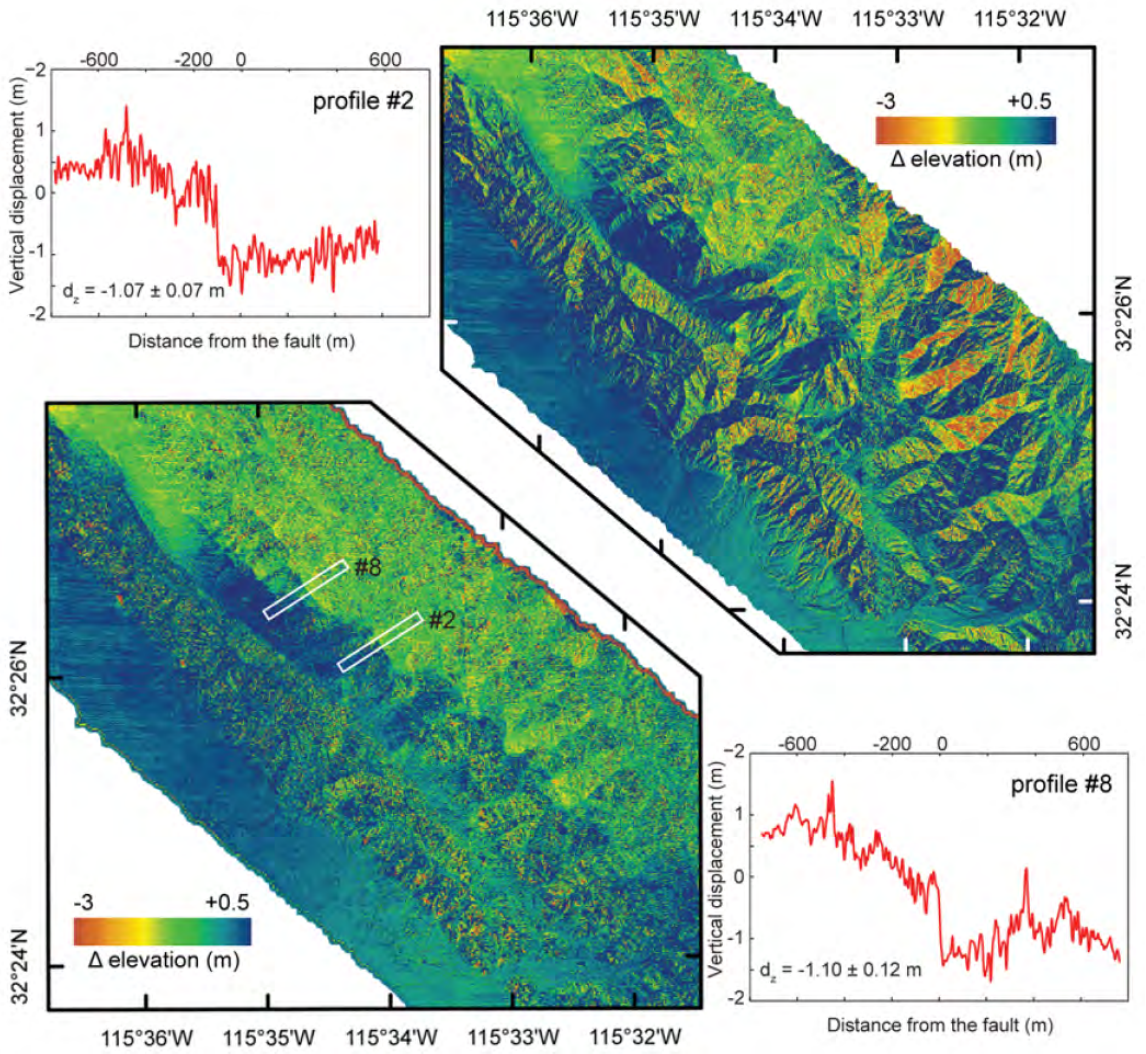

Figure 23. Pre and post earthquake LiDAR difference around the Puerta Accomodation zone of the 2010 El Mayor Cucapah earthquake. Top-right: before 2D image matching correction. The fault rupture cannot be seen and signal is overwhelmed by topographic artifacts. Lower-left: Pre and post-earthquake LiDAR difference once 2D image matching is applied to compensate for lateral offsets. The en-echelon pattern is clearly visible and surface rupture can be quantified from the corresponding profiles (upper-left and lower-right).

match the two surfaces, potentially leading to erroneous matches. A potential solution to this problem is to embed the ICP, or any other similarity criteria, into a global matching framework with regularization. Matching the two topography surfaces globally with constraints on the 3D offset field has given the best results thus far with a guarantee to find a globally optimal solution to the deformation problem. However, the complexity of such an algorithm still makes it impractical for large datasets.

Image matching trends, accuracy and measurement density

The image matching results presented above have mostly been achieved using so-called local methods, meaning that the matching problem is solved on

localized data patches, independent of the matching result from neighboring patches. The computer vision community (Scharstein and Szeliski, 2002) has long shown that a global regularization of the matching problem allows for better results, but these techniques are still seldom used on remote sensing data because of the complexity in processing large datasets. However, semi-global matching (SGM) approaches have recently been popularized by Hirschmuller (2005) and by an open source implementation, Micmac (Pierrot-Deseilligny and Paparoditis, 2006), for stereo extraction. At a fraction of the complexity of global matching regularization, SGM achieves a good compromise with performance.

Recent studies are still pushing the development of global optimization methods, in particular to merge elevation models extracted from several stereo pairs, or to better account for occlusions in data. For instance, the newest advances on fast solvers based on primal-dual schemes are now making global optimization methods attractive even for large datasets (Conejo et al. 2014b). Other studies have also shown that the commonly used techniques to lower the matching complexity, based on image pyramidal schemes where the images to be matched are down-sampled and matched at each level, are non-optimal with no proof of convergence to the desired objective. Instead, energy pyramids, where the energy to be minimized is down-sampled, have proven to be the correct representation of the problem, leading to enhanced details in the reconstructed elevation data (Conejo et al. 2014a). Together, these new techniques can be beneficial for the processing of multi-stereo gazing imagery, but also for the processing of LiDAR data. They can help detecting changes due to building collapse, or changes due to ground deformation (Figure 24).

Processing speed and data volume for new systems

In order to produce better elevation models, a current trend has been to take advantage of cheaper hardware to collect more images with higher variety of incidence angles at higher resolution. A direct example is the proliferation of small uninhabited aerial vehicles (sUAVs), which can take advantage of Structure from Motion (SfM) algorithms. Circling around a point of interest and acquiring a multitude of images allows the reduction of occlusion problems, and the low flight altitude allows very high-resolution images to be acquired. Therefore, constraint on the topographic extraction algorithms can be relaxed as the redundancy of data compensates for the need of more complex algorithms. The deployment of Wide Area Motion Imagery (WAMI) sensors, which can acquire large area video at high resolution using high altitude planes, is another example of these new systems being available. These new systems produce a tremendous amount of data, and algorithms need to be faster to handle the large increase in data volume. It is also likely that if the local matching methods might suffice to generate quick qualitative results, the global optimization methods will deliver better measurement of ground elevation and changes. For these reasons, the global optimization methods have the challenge to adapt to even larger data volume. By delivering better results on fewer data, they could also contribute in finding the best compromise between the volume of data collected and the complexity of the algorithm for a given measurement performance.

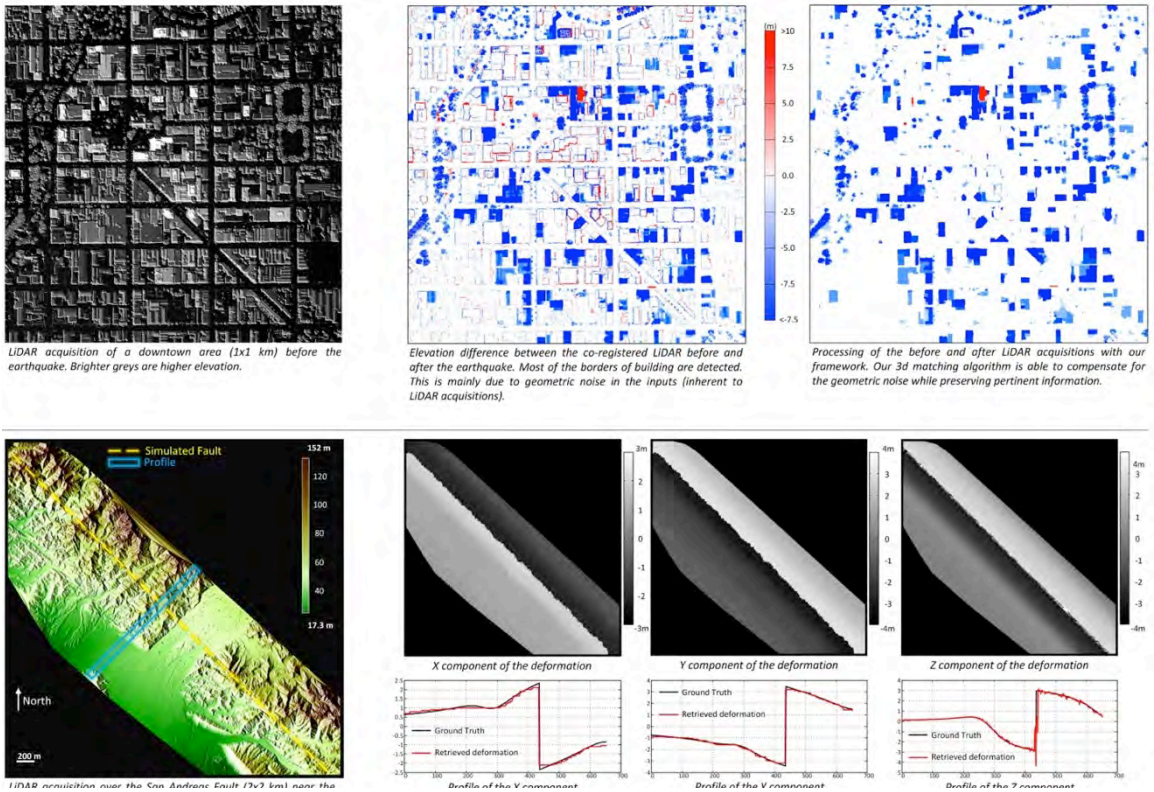

Figure 24. (Top row) The matching framework from Conejo et al (2014a) was used to compare changes between two urban LiDAR images acquired above the city of Christchurch before and after the 2011 earthquake that produced damages to buildings. Differencing the LiDAR brings out many artifacts, in particular at the edges of the buildings, where the LiDAR data may not align very well, or might be noisy due to shadowing. After applying the 3D matching framework and solving for local displacement of each LiDAR point in x,y,z, the z component represents the regularized elevation change and is robust against detection errors. (Bottom row) We simulated an earthquake using a simple Okada dislocation model and applied it to a piece of LiDAR from the USGS B4 data. The 3D matching was able to nicely recover the deformation field applied in the three dimensions with good accuracy despite the L1 norm gradient regularization of the algorithm (Conejo at al, 2013).

At the time of the workshop, the attendees agreed that using the current passive optical systems (UAV, airborne, or spaceborne) and using the current algorithms (local or global matching), the best elevation and measurement accuracy that can consistently be achieved seems to be on the order of 15-50 cm, with processing times that can potentially last for over a day depending on the size of the dataset in the area of interest.

Visualization of Observations and Simulations

Storing, transporting, analyzing, and visualizing rapidly growing quantities of data is a significant challenge for astronomy and particularly for high resolution space based gazing systems. To tackle this problem, the Jet Propulsion Laboratory's Research and Technology Development Astronomy Big Data Initiative uses the Automated Movie Production Environment, alert, Display and distribution (AMPED) pipeline to create movies of these large data sets. AMPED is used for storing, transporting, analyzing, and visualizing rapidly growing

quantities of observation and simulation data. It is the visualization component of the Jet Propulsion Laboratory's Research and Technology Development Astronomy Big Data Initiative that aims to enhance dataset usage through "movie" visualization.

Space observations and simulations include complex sets of parameters that change with time or other independent parameters, and the analysis of these datasets is greatly enhanced through "movie"-style visualizations. The AMPED system uses new event and feature detection codes, metadata-driven procedures, and custom search and pattern recognition algorithms to create movies from astronomy simulation and observation datasets. In so doing, AMPED helps scientists visualize mission operations, observations, features, targets, and dynamic processes. The system's inputs include mission plans, spacecraft commands, feature catalogs, models, simulations, observations, metadata, and events. It exploits expert knowledge to create time-, feature-, and event-driven algorithms and procedures.

AMPED movies enable rapid comparison of observations and models at a variety of temporal-spatial scales and viewpoints. Scientists can watch changes that occur over decades, centuries, millennia, and geologic epochs in a few minutes on screen. Frames can be sped up, slowed down, edited, repeated, and looped to focus on particular events. Vertical, horizontal, and temporal scales can be exaggerated to enhance small-scale features. Infrared and radar observations can be mapped into the visible spectrum, with the ability to modify the contrast, intensity, color, hue, and saturation to highlight differences.

Experimental data records (EDRs) and reduced data records (RDRs) contain instrument observations and metadata and are stored in a variety of formats. EDR and RDR metadata contains hundreds to thousands of unique parameter equal-value pairs. Metadata parameters include observation time and date, spatial-temporal reference data, illumination angle, instrument pointing, and field of view. AMPED includes a file transformation (FileTrans) code that automatically translates files from one EDR/RDR format to another. This code also creates multiple versions of AMPED movies for distribution.

Figure 25 shows a single frame from an AMPED movie that simulates a flight over the Mojave Crater on Mars. The virtual camera's altitude is approximately 3 kilometers above the Martian surface. A 3D model of this crater was created from a stereo pair of Mars Reconnaissance Orbiter (MRO) High-Resolution Imaging Science Experiment (HiRISE) observations of Mojave crater. The MRO spacecraft has collected more than 200 Tbits of scientific data as it orbits 300 kilometers above Mars' surface. The 3D model's image resolution is 25 centimeters/pixel, which enables scientists to explore the details and dynamics of geologic features including: polar caps, volcanoes, craters, dunes, valleys, lakebeds and river networks.

AMPED connects astronomers to space- and ground-based observations, numerical models, simulations, advanced computer graphic visualization, and image-processing and analysis tools. The AMPED pipeline has been adapted to

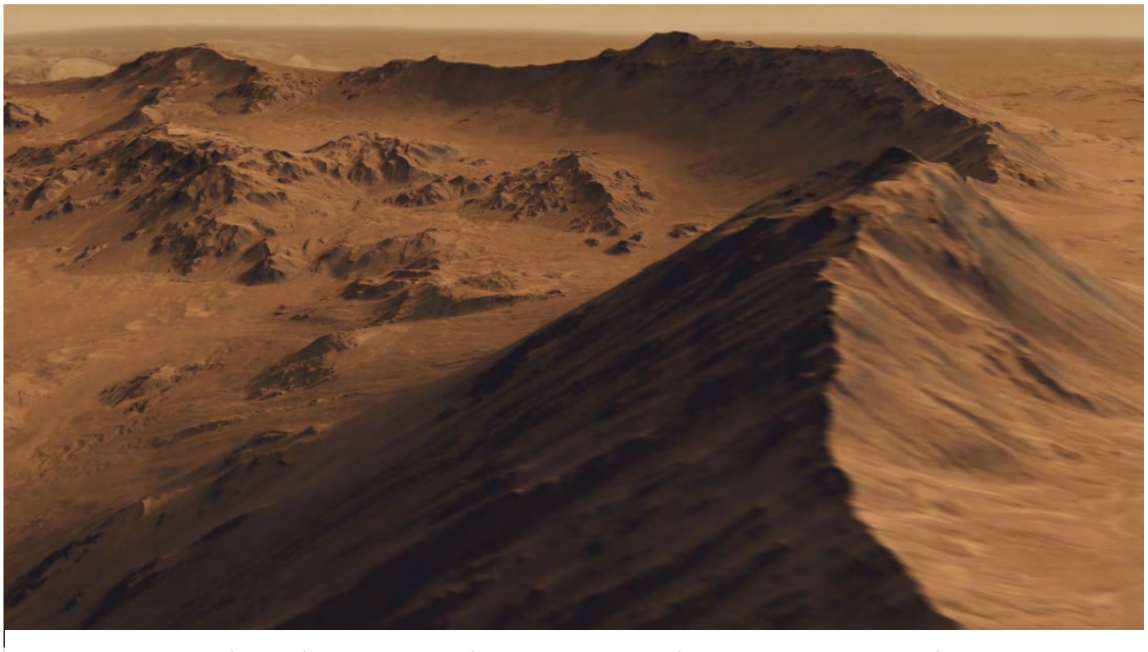

Figure 25. A single frame from a high-definition simulated flight over the Mojave Crater on Mars. The frame is based on stereo images taken by the High-Resolution Imaging Science Experiment (HiRISE) camera on NASA's Mars Reconnaissance Orbiter.

support several National Aeronautics and Space Administration (NASA) Space and Earth science missions. In the last year the AMPED pipeline was used to create movies for: Juno, MRO, Solar and Terrestrial Relations Observatory (STEREO), Opportunity rover and Mars Science Laboratory (MSL) Curiosity rover. AMPED movies are delivered online to science team members, museums, planetariums, science centers, mission and social media websites.

Design Space

The driving measurements that are not addressed by current assets are dynamic, high resolution (1m horizontal, 0.1m vertical), surface models from multi-angle imagery acquired globally and refreshed at a 5-day cadence with some degree of multi-spectral capability. The resulting data products would be global time-stamped ("4D") feature catalogs of "discrete" dynamic objects like dunes, icebergs, landslides, avalanches, or lakes. DSMs enable more robust detection/cataloging and characterization (e.g., dune volume, iceberg volume over time) than simple 2D imagery. Time-series of derived attributes should also be provided. Tools are needed to help scientists utilize such data to address their questions. Data products include mass transfer (flux) analysis - snowmelt, landslides, glaciers, shorelines, sand redistribution, vegetation, etc. Analysis of sub-resolution surface roughness via BRDF is required. The imager could be used for pre-hazard risk assessment, and post-hazard evaluation and triage.

The ideal design space makes use of a multisensory configuration. Small UAVs (sUAVs) can be used to develop high-resolution models using low-cost equipment and sensors. They are ideally suited for imaging areas beneath overhanging structures such as bridges or under overhanging outcrops. sUAVs can complement space-based remote sensing, particularly in that they are portable and can be used to respond rapidly to events. They are easy to maintain, deploy, and upgrade. At present sUAVs are limited by endurance, legality of flight, payload capability, and weather.

A spaceborne gazing imager should have a resolution of <1 m with a field of view of >1 km. Placing the instrument in a non-sun-synchronous orbit enables the BRDF retrievals. Angle diversity should be ±60° with at least 15 measurements distributed over that range of angles. The instrument should be capable of collecting video during a pass. Multispectral measurements are required to study material properties. Ideally, the measurements would go out into the near-IR range.

If we disregard the thermal imaging aspects that are driven by desire for volcano, levee, and fire measurements, these objectives could be largely met with a high-resolution multispectral imaging platform. The inclination will have to be tuned to maximize the desired target distribution. Depending upon the altitude of the system the diameter may be in the 30-60 cm class. By conducting a fixed-point stare collection, a large array of angles can be sampled during each pass. If multispectral imaging is a driving need, a slow-scanning pushbroom configuration may be considered. The ultimate configuration along these lines may look like a large version of MISR with 3-5 telescopes that employ pushbroom imaging. Using a slower scan enables a higher Q to maintain both high resolution and good imaging SNR across all bands.

Table 4. A reduction of the measurement needs by discipline (Table 3) along with candidate system design parameters

Measurement Objective	Design Parameter
DEM Spatial Resolution: 0.5m or better	30-60cm Telescope at 400-600km Orbit
DEM Vertical Resolution: 0.1m or better	10-20 view angles in a pass
Field of View: >1km	2k x 2k FPAs or better, 0.1 - 0.2 degree FOV
BDRF and Albedo Retrieval	Multiple view angles, multiple sun angles
Texture Parameters	Multiple view angles, multiple sun angles
Displacement and Velocity distributions	Minutes of dwell, multiple passes in close succession (< 1 week)
Volumetric Changes	Repeated DEM retrievals
Worldwide sampling with repeat cadences of 5-14 days	Non-sun-synchronous orbit included to maximize target coverage
Surface Material Classification	Mutlispectral Imaging
Evolution of temperature with time	Thermal Imaging (potentially with sounding for absolute temp calibration)

Products

- Better 3D - diversity of angles
- BRDF - multiangle
- Texture (can extrapolate into sub-pixel scale)
- Video - frame rate or multiangles for 3D models
- Spectral bands
- Thermal maps and evolution of temperature with time
- Displacement/velocity field
- Need metadata
- Public outreach
- Toolbox of analysis techniques for common workflow

Conclusions and Recommendations

Gazing imaging can address a wide range of applications that fall into the broad categories of climate change, natural hazards, and planetary processes. A substantial strength of the gazing approach is that coarse and fine structure, material properties, and surface reflectance can be simultaneously measured. This allows for separation of forcings and deeper understanding for a variety of processes.

Recommendation 1: The applications and benefits of gazing imaging should be considered in the upcoming National Research Council Earth Science Decadal Survey. Because the range of applications is so broad, a gazing imaging system would make an excellent facility-type instrument for diverse studies.

Recommendation 2: The development of gazing imaging instruments and algorithms should be done in a coordinated manner. In this way a true tiered system can be developed that makes use of small UAVs, airborne instruments, and spaceborne assets. This approach also allows for acquisition of surrogate data for spaceborne systems prior to development.

Recommendation 3: Partnerships with commercial imaging companies, such as Skybox, should be developed. Opportunities to serve the science community and develop new approaches should be explored.

Recommendation 4: A dedicated space instrument could be envisioned as a frame imager with multiple cameras to insure global and permanent multi-stereo coverage. Indeed, repeat high-resolution stereo mapping has been identified in this study as one of the most important products to be derived from a gazing system. Because of occlusion problems, it was shown that standard stereo imagery is often inadequate in places of high interest such as rugged alpine areas with debris-covered glaciers, volcanoes, steep slopes with landslides, or buildings for disaster response. A spacecraft carrying at least three instruments with about 15 degrees separation would be ideal to derive time-series of high accuracy topography in most places of interest. Each of these cameras could be augmented with multi-spectral sensors to probe the physical characteristics of the ground and pave the way to more systematic BRDF studies. Whenever required, this instrument could be steered in order to provide higher angle density and more persistent imaging. The redundancy of the camera systems would allow acquiring image cubes with high angle density, while requiring only slight spacecraft rotation. This configuration would allow the spacecraft to save valuable orbit time and potentially image more targets and to do so more efficiently. Indeed, the main reason commercial satellites cannot be used in practice as gazing scientific instruments, although the capability may actually exist, is that gazing requires the use of a large part of an orbit to be dedicated to a given study site, making gazing too expensive for standard commercial practices.

References

Arrowsmith, J R., and Zielke, O., Tectonic geomorphology of the San Andreas Fault zone from high resolution topography: an example from the Cholame segment, Geomorphology, doi:10.1016/j.geomorph.2009.01.002, 2009.

Barnett T.P., J.C. Adam, D.P. Lettenmaier (2005), Potential impacts of a warming climate on water availability in snow-dominated regions. Nature, 438, 303–309.

Barnhart, K. R., R. S. Anderson, I. Overeem, C. Wobus, G. D. Clow, and F. E. Urban (2014), Modeling erosion of ice-rich permafrost bluffs along the Alaskan Beaufort Sea coast, J. Geophys. Res. Earth Surf., 119, 1155–1179, doi:10.1002/2013JF002845.

Bhattachan, A., D'Odorico, P., Baddock, M., Zobeck, T.M., Okin, G.S., Cassar, N., 2012. The Southern Kalahari: a potential new dust source in the Southern Hemisphere? Environmental Research Letters 7, 024001.

Bridges NT, et al. 2012. Earth-like sand fluxes on Mars. Nature 485(7398): 339–342.

Bridges, N.T., F. Ayoub, J-P. Avouac, S. Leprince, A. Lucas, and S. Mattson (2012), Earth-like sand fluxes on Mars, Nature, 485, 339-342.

Buades A, et al. 2008. Nonlocal image and movie denoising. International Journal of Computer Vision 76(2): 123–139.

Conejo, B., N. Komodakis, S. Leprince, and J.P Avouac. Speeding-up Graphical Model Optimization via a Coarse-to-fine Cascade of Pruning Classifiers. Advances in Neural Information Processing Systems 27, 2014b.

Conejo, B., S. Leprince, F. Ayoub, and J.P Avouac “A 2D and 3D registration framework for remote-sensing data,” Abstract G33A-0971 presented at 2013, Fall Meeting, AGU, San Francisco, CA, 9-13 December.

Conejo, B., S. Leprince, F. Ayoub, and J.P Avouac “Fast Global Stereo Matching via Energy Pyramid Minimization”, Photogrammetric Computer Vision Symposium - PCV2014, 2014a.

Crouvi, O., Schepanski, K., Amit, R., Gillespie, A.R., Enzel, Y., 2012. Multiple dust sources in the Sahara Desert: The importance of sand dunes. Geophys. Res. Lett. 39, L13401.

De Michele M, et al. 2012. Direct measurement of ocean waves velocity field from a single SPOT-5 dataset. Remote Sensing of Environment 119: 266–271.

Deems, J. S., T. H. Painter, and D. C. Finnegan (2013), Lidar measurement of snow depth: a review, J. Glaciol., 59(215), 467–479, doi:10.3189/2013JoG12J154.

Deems, J. S., T. H. Painter, and D. C. Finnegan (2013), Lidar measurement of snow depth: a review, J. Glaciol., 59(215), 467–479, doi:10.3189/2013JoG12J154.

Donnellan, A., J. Parker, S. Hensley, M. Pierce, J. Wang, J. Rundle, UAVSAR Observations of Triggered Slip on the Imperial, Superstition Hills, and East Elmore Ranch Faults Associated with the 2010 M 7.2 El Mayor - Cucapah Earthquake, Geochemistry, Geophysics, Geosystems, 15, doi: 10.1002/2013GC005120, 2014.

Dumont, M., O. Brissaud, G. Picard, B. Schmitt, J.-C. Gallet, and Y. Arnaud, "High-accuracy measurements of snow Bidirectional Reflectance Distribution Function at visible and NIR wavelengths – comparison with modeling results," Atmos. Chem. Phys. 10 (2010): pp. 2507-20.

Dyurgerov, M. (2003), Mountain and subpolar glaciers show an increase in sensitivity to climate warming and intensification of the water cycle, J. Hydro., 282, 164–176.

Fletcher, J.M., O.J. Teran, T.K. Rockwell, M.E. Oskin, K.W. Hudnut, K.J. Mueller, R.M. Spelz, S.O. Akciz, E. Masana, G. Faneros, E.J. Fielding, S. Leprince, A.E. Morelan, J. Stock, D.K. Lynch, A.J. Elliott, P. Gold, J. Liu-Zeng, A. González-Ortega, A. Hinojosa-Corona1, and J. González-García (2014), Assembly of a large earthquake from a complex fault system: Surface rupture kinematics of the 4 April 2010 El Mayor–Cucapah (Mexico) Mw 7.2 earthquake, Geosphere, 10.1130/GES00933.1.

Frankel, K.L., Dolan, J.F., Owen, L.A., Finkel, R.C., and Hoeft, J.S. (2007). Spatial variations in slip rate along the Death Valley-Fish Lake Valley fault system from LiDAR topographic data and cosmogenic 10Be geochronology: Geophysical Research Letters, v. 34, doi:10.1029/2007GL030549.

Gardner, A.S., G. Moholdt, J. Graham Cogley, B. Wouters, A.A. Arendt, J. Wahr, E. Berthier, R. Hock, W. Tad Pfeffer, G. Kaser, S.R.M. Ligtenber, T. Bolch, M.J. Sharp, J. Ove Hagen, M. R. van den Broeke, F. Paul (2013), A reconciled estimate of glacier contributions to sea level rise: 2003 to 2009, Science, 340, 852–857, DOI: 10.1126/science.1234532.

Hesp, P.A., Walker, I.J., 2013. 11.17 Coastal Dunes, in: Shroder, J.F. (Ed.), Treatise on Geomorphology. Academic Press, San Diego, pp. 328-355.

Hilley, G. E., and Arrowsmith J R. (2008). Geomorphic response to uplift along the Dragon's Back pressure ridge, Carrizo Plain, California, Geology, v. 36; no. 5; p. 367–370; doi: 10.1130/G24517A.1.

Hirschmuller H 2005. Accurate and efficient stereo processing by semi-global matching and mutual information. In: Schmid C, et al. (eds.), 2005 IEEE Computer Society Conference on Computer Vision and Pattern Recognition, Vol. 2, Proceedings, pp. 807–814.

Hudnut, K.W., Borsa, A., Glennie, C., and Minster, J.B. (2002). High-resolution topography along surface rupture of the 16 October 1999 Hector mine,

California, earthquake (Mw 7.1) from airborne laser swath mapping. Seismological Society of America Bulletin, v. 92, p. 1570–1576, doi: 10.1785/0120000934.

Hurst, M. D, Mudd, S. M. Attal, M., Hilley, G. (2013). Hillslopes record the growth and decay of landscapes, Science, 341, 868-871, doi:10.1126/science.1241791.

Intergovernmental Panel on Climate Change (IPCC) (2013), Climate Change 2013: The Physical Science Basis. Contribution of Working Group I to the Fifth Assessment Report of the Intergovernmental Panel on Climate Change, edited by T. F. Stocker et al., 1535 pp., Cambridge Univ. Press, Cambridge, U. K.

Joughin, I., S. B. Das, M. A. King, B. E. Smith, I. M. Howat, and T. Moon (2008), Seasonal Speedup Along the Western Flank of the Greenland Ice Sheet, Science, 320, 781–783, doi:10.1126/science.1153288.

Kääb A. and Leprince S. 2014. Motion detection using near-simultaneous satellite acquisitions. Remote Sensing of Environment, 154,164-179.

Kattenhorn and Prockter, 2014.

Kjeldsen, K. K., J. Mortensen, J. Bendtsen, D. Petersen, K. Lennert, and S. Rysgaard (2014), Ice-dammed lake drainage cools and raises surface salinities in a tidewater outlet glacier fjord, west Greenland, J. Geophys. Res. Earth Surf., 119, 1310–1321, doi:10.1002/2013JF003034

Klok, E.J., Greuell, Greuell, W. Oerlemans, J. 2003, “Temporal and spatial variation of the surface albedo of Morteratschgletscher, Switzerland, as derived from 12 Landsat images,” J. Glaciology, 49, 491-502, DOI: 10.3189/172756503781830395.

Langridge, R.M.; Ries, W.F.; Farrier, T.; Barth, N.C.; Khajavi, N.; De Pascale, G.P. (2014). Developing sub 5-m LiDAR DEMs for forested sections of the Alpine and Hope faults, South Island, New Zealand : implications for structural interpretations. Journal of Structural Geology, 64: 53-66; doi: 10.1016/j.jsg.2013.11.007.

Leprince S, et al. 2007. Automatic and precise orthorectification, coregistration, and subpixel correlation of satellite images, application to ground deformation measurements. IEEE Transactions on Geoscience and Remote Sensing 45(6): 1529–1558.

Leprince S, et al. 2008. Monitoring earth surface dynamics with optical imagery. Eos, Transactions American Geophysical Union 89(1).

Michel R, et al. 2013. A geostationary optical seismometer, proof of concept. IEEE Transactions on Geoscience and Remote Sensing 51(1): 695–703.

Milliner, C., Dolan, J.F., Hollingsworth, J., Leprince, S., Ayoub F., Sammis, C. (2015), Quantifying near-field and off-fault deformation patterns of the 1992

Mw 7.3 Landers 1 earthquake, Geochem, Geophys., Geosys., DOI: 10.1002/2014GC005693

Motyka, R. J., W. P. Dryer, J. Amundson, M. Truffer, and M. Fahnestock (2013), Rapid submarine melting driven by subglacial discharge, LeConte Glacier, Alaska, Geophys. Res. Lett., 40, doi:10.1002/grl.51011.

Necsoiu M, et al. 2009. Monitoring migration rates of an active subarctic dune field using optical imagery. Remote Sensing of Environment 113(11): 2441–2447.

Nicholson, S.E., 2000. Land surface processes and the Sahel climate. Reviews of Geophysics 39, 117.

Nissen E, et al. 2012. Three-dimensional surface displacements and rotations from differencing pre- and post-earthquake LiDAR point clouds. Geophysical Research Letters 39.

Parajuli, S. P., Z.-L. Yang, and G. Kocurek (2014), Mapping erodibility in dust source regions based on geomorphology, meteorology, and remote sensing, J. Geophys. Res. Earth Surf., 119, doi:10.1002/2014JF003095.

Pierrot-Deseilligny M and Paparoditis N 2006. A multiresolution and optimizationbased image matching approach: An application to surface reconstruction from SPOT5-HRS stereo imagery. In: ISPRS Workshop on Topographic Mapping from Space (With Special Emphasis on Small Satellites) Ankara: IAPRS.

Pritchard, H. D., R. J. Arthern, D. G. Vaughan, and L. A. Edwards (2009), Extensive dynamic thinning on the margins of the Greenland and Antarctic ice sheets, Nature, 461(7266), 971–975, doi:10.1038/nature08471.

Rignot, E. et al. (2010), Rapid submarine melting of the calving faces of West Greenland glaciers, Nature Geosci., 3, 187–191.

Rignot, E., I. Velicogna, M. Van den Broeke, A. Monaghan, and J. Lenaerts (2011), Acceleration of the contribution of the Greenland and Antarctic ice sheets to sea level rise, Geophys. Res. Lett., 38(5), L05503.

Rymer, M.J., J.A. Treiman, K.J. Kendrick, J.J. Lienkaemper, R.J. Weldon, R. Bilham, M. Wei, E.J. Fielding, J.L. Hernandez, B.P.E. Olson, P.J. Irvine, N. Knepprath, R.R. Sickler, X.Tong, and M.E. Siem, (2011), Triggered Surface Slips in Southern California Associated with the 2010 El Mayor – Cucapah, Baja California, Mexico Earthquake, U.S. Geological Survey Open-File Report 2010-1333 and California Geological Survey Special Report 221, 62 p., available at http://pubs.usgs.gov/of/ 2010/1333/.

Salisbury, J. B., Rockwell, T. K., Middleton, T. J., Hudnut, K. W., (2012). LiDAR and Field Observations of Slip Distribution for the Most Recent Surface Ruptures along the Central San Jacinto Fault. Bulletin of the Seismological Society of America, 102 (2): 598 DOI: 10.1785/0120110068.

Scambos TA, et al. 1992. Application of image cross-correlation to the measurement of glacier velocity using satellite image data. Remote Sensing of Environment 42(3): 177–186.

Scambos, T., et al. (2008). Calving and ice-shelf break-up processes investigated by proxy: Antarctic tabular iceberg evolution during northward drift. J. Glac., 54, 579–591.

Scharstein, D. and Szeliski, R 2002. A taxonomy and evaluation of dense two-frame stereo correspondence algorithms, International journal of computer vision 47 (1-3), 7-42

Scherler D, et al. 2008. Glacier-surface velocities in alpine terrain from optical satellite imagery—Accuracy improvement and quality assessment. Remote Sensing of Environment 112(10): 3806–3819.

Scherler D, et al. 2011. Spatially variable response of Himalayan glaciers to climate change affected by debris cover. Nature Geoscience 4(3): 156–159.

Suncar, O., Rathje, E.M., and Buckley, S. 2013. Deformations of a Rapidly Moving Landslide from High-Resolution Optical Satellite Imagery, *GeoCongress 2013: Stability and Performance of Slopes and Embankments III*, San Diego, CA, March.

Thomas, D.S.G., Wiggs, G.F.S., 2008. Aeolian system responses to global change: challenges of scale, process, and temporal integration. Earth Surface Processes and Landforms 33, 1396-1418.

Tsvetsinskaya, E.A., Schaaf, C.B., Gao, F., Strahler, A.H., Dickinson, R.E., Zeng, X., Lucht, W., 2002. Relating MODIS-derived surface albedo to soils and rock types over Northern Africa and the Arabian peninsula. Geophysical Research Letters 29.

Van Puymbroeck N, et al. 2000. Measuring earthquakes from optical satellite images.Applied Optics 39(20): 3486–3494.

Vermeesch P and Drake N 2008. Remotely sensed dune celerity and sand flux measurements of the world's fastest barchans (Bodele, Chad). Geophysical Research Letters 35(24). http://dx.doi.org/10.1029/2008g/035921.

Watson, A., 1990. The control of blowing sand and mobile desert dunes, in: Goudie, A.S. (Ed.), Techniques for Desert Reclamation. John Wiley & Sons Ltd., Chichester, pp. 35-85.

Wolf PR and Dewitt BA (2000) Elements of Photogrammetry with Application in GIS, 3rd edn. India: McGraw-Hill Education.

Worldview, 2014. http://www.digitalglobe.com/products/information.

Yizhaq, H., Askenazy, Y., Tsoar, H., 2008. Sand dune dynamics and climate change: a modeling approach. Journal of Geophyical Research 114.

Zielke, O., Arrowsmith, J. R., Ludwig, L. G., & Akçiz, S. O. (2010). Slip in the 1857 and earlier large earthquakes along the Carrizo Plain, San Andreas fault. Science, 327(5969), 1119-1122.

Acronyms

DEM – Digital Elevation Model

DSM – Digital Surface Model

FPA – Focal Plane Array

ISS – International Space Station

MSI – Multispectral Imaging

MWIR – Mid-wavelength Infrared

NIR – Near Infrared

PAN – Panchromatic

ROI – Region of Interest

SfM – Structure from Motion

SNR – Signal to Noise Ratio

sUAV – Small Uninhabited Aerial Vehicle

SWIR – Short Wavelength Infrared

TDI – Time Delay Integration

TIR – Thermal Infrared

VNIR – Very Near Infrared

WAMI – Wide Area Motion Imagery

Appendix: Specific Identified Areas of Interest

The following table highlights specific scientific interests outlined by the workshop participants.

Science Interest, Question, Problem (Interested participant)	Current Technology Approach	Gazing Approach
Predicting liquefaction-induced displacements (Rathje)	2D image correlation to get horizontal displacements; aerial or ground based observation of changes in distribution of surface water, such as ponding, as a proxy for uplift and subsidence (in the case of areas with formerly horizontal agricultural fields)	??? Better 3D model with cm level deformation. Rapid response
earthquake fault mechanics (Donnellan, Stock)	Crustal deformation from GPS (spatially sparse) and InSAR (temporally sparse and decorrelated near fault)	Measure fault zone - disruption, coseismic and afterslip. What is happening on the short timescale after large earthquakes. Aftershocks and deformation. Triggered slip on adjacent faults, might be delayed by several or up to 12 hours. Aseismic processes in adjacent regions.
-fjord circulation -iceberg movement -ice-ocean interactions -Iceberg melt rates -Timescales of response of ocean and ice (Sutherland)	-in situ observations -gps units -imagery (modis, worldview, etc)	-velocity maps of near terminus water/ice (on 5-10 minute time scales and synoptic timescales) - vertical motion (melting) of icebergs (rough magnitude is 1 meter/day, so over a month that's 30 m or about 3 m of freeboard change you'd need to resolve) -ability to get inaccessible regions and scale up process studies
post-disaster reconnaissance; infrastructure monitoring and inspection Liquefaction Including monitoring aging infrastructure (Franke)	- UAV-based remote sensing - terrestrial remote sensing (eg, lidar) - manual inspection	- rapid anomaly detection with 2D object recognition - 3D reconstruction of larger areas (>1km2)...cm displacement detection would be ideal - routine monitoring of large infrastructure objects (levees or pipelines)Super-resolution -6-12 month revisit except during floods - multiple times per day - thermal imaging on levees - the ability to accurately detect ground displacements <5cm in size would constitute a significant milestone. - UAV/satellite coupled imagery and sensing (single or multi-sensor)

Science Interest, Question, Problem (Interested participant)	Current Technology Approach	Gazing Approach
Composition and physical structure of surface. Degree of snow/ice contamination. Albedo and relationship between solar power input and ice mass loss in glaciers. (Goguen)	Assume BRDF topography and roughness is poorly known. Integrate assumed BRDF to get albedo.	Gazing provides independent determination of topography (roughness larger than DEM resolution). Unresolved roughness will still influence photometry and will be part of BRDF for each resolved surface element. Each resolution element will have n measurements of BRDF where n is the number of images used to generate the DEM. DEM changes measure ice volume lost.
Rates and episodicity of plate boundary motions at subaerial ridge (extensional plate boundary) systems (Iceland, Afar); how fast do dikes intrude along and across the rift system? (Stock)	InSAR, GPS (sparse networks), field observations on the ground (still useful and important to do, although logistically difficult, especially in East Africa), local microseismic surveys	Observe short timescale deformation during several months of dike intrusion or volcanism; need <1 m pixel size to see 1 m wide dike intrusion reflected in active faulting at the surface. Rapid response requires deployment and maintenance of local seismometers.
Dynamics of sand dunes; sediment flux in relation to boundary conditions (Lancaster) Dust emissions in relation to surface characteristics (e.g. moisture, veg cover, roughness) (Lancaster)	repeat imaging and high-res DEM combine with wind measurements or models Combine with aerosol measurements (e.g. aerosol optical depth)	event scale changes and fluxes Changes in volume on seasonal scales Target dust hotspots for staring event scale processes Identification of precursor conditions, spatial variability of emission sites
Landslide dynamics and hazard (Allstadt) Seismically induced landslide hazard (Allstadt) Volcano monitoring (Allstadt)	seismic recordings, static pre- and post-slide images, lidar, radar interferometry, GPS, lab tests, numerical modeling seismic monitoring, GPS, gas monitoring, static satellite images, InSAR (field instrumentation can be dangerous and very difficult)	-post-quake inventories of triggered landslides using detailed DEM's in areas of steep terrain & improved empirical relations for assessing future hazard -capture long term landsliding processes (scaling size/volume etc.) in dynamic places (stratovolcanoes, steep mountains) -identifying areas of precursory crack growth/accelerating crack growth that could be approaching failure -survey known slow moving landslides -rapid near real-time identification of areas affected by seismically induced landsliding for guiding response efforts seismic monitoring can alert to when to target a certain volcano, measure slow deformation, capture dynamic processes like explosions, pyroclastic flows,

Science Interest, Question, Problem (Interested participant)	Current Technology Approach	Gazing Approach
Earthquake swarms and accompanying deformation (e.g. episodic tremor and slip) (Allstadt)		landslides, lava flows at high res. in steep terrain
Vegetation Canopy height Biomass Disease evolution recovery from fire deforestation (Mushkin)	LiDAR Landsat ASTER stereo Multispectral/ hyperspectral imaging such as AVIRIS for discrimination of different plant species	sub-pixel roughness Deforestation where saturation occurs with other instruments
Volcanoes Dome emplacement/growth Caldera uplift/subsidence Dynamics of evolution of surface of tube-fed lavas (e.g., Hawaii) Mushkin)	Time-lapse cameras Airborne photogrammetry Leveling lines tiltmeter	3D timeseries w/ minimal occlusion Volume change
Glaciers and climate change Snow coverage (Scherler)	MODIS - daily and global with low spatial resolution. Can make global assessments Landsat - long time history and area changes ICESAT for elevation changes for Greenland and Antarctica Field work - stakes in easily accessible areas	Better spatial resolution Target inaccessible areas Comprehensive coverage Benchmark places - stare at hotspots: snow avalanches, mass changes Dynamics of time periods up to years Volume changes water Understanding potential energy of glacier surface Seasonal snow coverage - 10 cm - 1 m Fjords with calving - cliff retreats 1-10 m/yr Debris - boulder scale of 10-50 cm
Dynamics and variability of outlet glaciers, ice streams Sub ice shelf melting: location, timing, magnitude Mountain glacier mass balance Snowpack evolution	High-res Commercial Satellite Stereo Imagery Satellite InSAR Airborne LiDAR Airborne DSLR SfM UAV SfM	Additional DEMs to populate timeseries during critical time periods (e.g. early summer calving/acceleration) Real-time velocity for >10 km/yr glaciers Real-time observations of calving events, inland response

Science Interest, Question, Problem (Interested participant)	Current Technology Approach	Gazing Approach
Subglacial fluvial processes/evolution (Shean)	GPS	Reconstruction of steep calving fronts (height above floatation) Glacier surging behavior
Sea ice evolution and dynamics (Shean)	ERS-1 and ERS-2 scatterometer and SAR data (radar and microwave) - scales 20 km (global) to 25 m (local); ICESAT 2 (coming up for launch in 2016?)	
Forest fires Seeing through smoke and debris Microclimates produced (Shean)		
tsunami (Shean)	coastal tide gauges	